RL-TR-91-351
In-House Report
December 1991

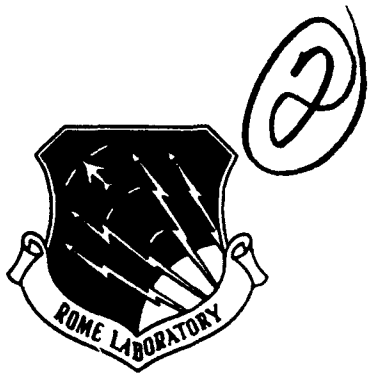

ANALYTICAL CHARACTERIZATION OF BISTATIC SCATTERING FROM GAUSSIAN DISTRIBUTED SURFACES

Lisa M. Sharpe

APPROVED FOR PUBLIC RELEASE; DISTRIBUTION UNLIMITED.

Rome Laboratory
Air Force Systems Command
Griffiss Air Force Base, NY 13441-5700

This report has been reviewed by the Rome Laboratory Public Affairs Office (PA) and is releasable to the National Technical Information Service (NTIS). At NTIS it will be releasable to the general public, including foreign nations.

RL-TR-91-351 has been reviewed and is approved for publication.

APPROVED: John F Lennon

JOHN F. LENNON, Chief
Applied Electromagnetics Division

FOR THE COMMANDER: John K Schindler

JOHN K. SCHINDLER, Director
Electromagnetics & Reliability Directorate

If your address has changed or if you wish to be removed from the Rome Laboratory mailing list, or if the addressee is no longer employed by your organization, please notify RL(ERCE) Hanscom AFB MA 01731-5000. This will assist us in maintaining a current mailing list.

Do not return copies of this report unless contractual obligations or notices on a specific document require that it be returned.

REPORT DOCUMENTATION PAGE

Form Approved
OMB No. 0704-0188

1. AGENCY USE ONLY (Leave blank)	2. REPORT DATE	3. REPORT TYPE AND DATES COVERED
	December 1991	In-house, Jan 91 to Jun 91

4. TITLE AND SUBTITLE
Analytical Characterization of Bistatic Scattering From Gaussian Distributed Surfaces

5. FUNDING NUMBERS
PR: 2305
TA: J4
WU: 09
PE: 61102F

6. AUTHOR(S)
Lisa M. Sharpe

7. PERFORMING ORGANIZATION NAME(S) AND ADDRESS(ES)
Rome Laboratory/ERCE
Hanscom AFB, MA 01731-5000

8. PERFORMING ORGANIZATION REPORT NUMBER
RL-TR-91-351

9. SPONSORING/MONITORING AGENCY NAME(S) AND ADDRESS(ES)

10. SPONSORING/MONITORING AGENCY REPORT NUMBER

11. SUPPLEMENTARY NOTES

12a. DISTRIBUTION/AVAILABILITY STATEMENT
Approved for public release; distribution unlimited

12b. DISTRIBUTION CODE

13. ABSTRACT (Maximum 200 words)

In a study by Papa and Woodworth, the mean and variance of the diffuse power scattered from a clutter cell were examined as a function of cell size for one-dimensionally rough surfaces. Their study was performed for horizontally polarized incident and scattered fields. In this report their work is expanded to include vertical and arbitrary linear polarization. Scattering statistics and polarization effects will be examined using a theoretical model based upon physical optics. The present study shows that as the size of the clutter cell is decreased the statistical distribution of the scattered power deviates from Rayleigh. Also, it is shown that the tilt angle of the incident linear polarization has little effect on the statistics of the scattered wave.

14. SUBJECT TERMS		15. NUMBER OF PAGES
Rough surface scattering Bistatic scattering	Scattering statistics	54
		16. PRICE CODE

17. SECURITY CLASSIFICATION OF REPORT	18. SECURITY CLASSIFICATION OF THIS PAGE	19. SECURITY CLASSIFICATION OF ABSTRACT	20. LIMITATION OF ABSTRACT
Unclassified	Unclassified	Unclassified	SAR

Contents

1. INTRODUCTION 1

2. THEORETICAL FORMULATION 4

3. VERTICAL POLARIZATION 8

4. ARBITRARY LINEAR POLARIZATION 33

5. CONCLUSIONS 35

REFERENCES 43

Illustrations

1. Rayleigh Distribution Functions 3

2. Scattering Geometry 4

3. Surface Geometry 6

4. a. Magnitudes of Horizontal Reflection Coefficients 10
   b. Phases of Horizontal Reflection Coefficients

5. a. Magnitudes of Vertical Reflection Coefficients 11
   b. Phases of Vertical Reflection Coefficients

6. Mean and Variance of Scattered Power for: 13

   a. $\theta_i = 30^o$, $\lambda = 0.25$ m, $\sigma = 0.2$, $L = 3T$, $\varepsilon = 30 + j2$
   b. $\theta_i = 30^o$, $\lambda = 0.25$ m, $\sigma = 0.2$, $L = 6T$, $\varepsilon = 30 + j2$
   c. $\theta_i = 30^o$, $\lambda = 0.25$ m, $\sigma = 0.2$, $L = 12T$, $\varepsilon = 30 + j2$

7. Mean and Variance of Scattered Power for: 14

   a. $\theta_i = 30^o$, $\lambda = 0.25$ m, $\sigma = 0.5$, $L = 3T$, $\varepsilon = 30 + j2$
   b. $\theta_i = 30^o$, $\lambda = 0.25$ m, $\sigma = 0.5$, $L = 6T$, $\varepsilon = 30 + j2$
   c. $\theta_i = 30^o$, $\lambda = 0.25$ m, $\sigma = 0.5$, $L = 12T$, $\varepsilon = 30 + j2$

8. Mean and Variance of Scattered Power for: 15

   a. $\theta_i = 75^o$, $\lambda = 0.25$ m, $\sigma = 0.5$, $L = 3T$, $\varepsilon = 30 + j2$
   b. $\theta_i = 75^o$, $\lambda = 0.25$ m, $\sigma = 0.5$, $L = 6T$, $\varepsilon = 30 + j2$
   c. $\theta_i = 75^o$, $\lambda = 0.25$ m, $\sigma = 0.5$, $L = 12T$, $\varepsilon = 30 + j2$

9. Mean and Variance of Scattered Power for H-pol for: 16

a. $\theta_i = 75°$, $\lambda = 0.25$ m, $\sigma = 0.5$, $L = 3T$, $\varepsilon = 30 + j2$
b. $\theta_i = 75°$, $\lambda = 0.25$ m, $\sigma = 0.5$, $L = 6T$, $\varepsilon = 30 + j2$
c. $\theta_i = 75°$, $\lambda = 0.25$ m, $\sigma = 0.5$, $L = 12T$, $\varepsilon = 30 + j2$

10. Mean and Variance of Scattered Power for: 17

a. $\theta_i = 75°$, $\lambda = 0.1$ m, $\sigma = 0.2$, $L = 3T$, $\varepsilon = 30 + j2$
b. $\theta_i = 75°$, $\lambda = 0.1$ m, $\sigma = 0.2$, $L = 6T$, $\varepsilon = 30 + j2$
c. $\theta_i = 75°$, $\lambda = 0.1$ m, $\sigma = 0.2$, $L = 12T$, $\varepsilon = 30 + j2$

11. Mean and Variance of Scattered Power for: 18

a. $\theta_i = 75°$, $\lambda = 0.1$ m, $\sigma = 0.5$, $L = 3T$, $\varepsilon = 80 + j9$
b. $\theta_i = 75°$, $\lambda = 0.1$ m, $\sigma = 0.5$, $L = 6T$, $\varepsilon = 80 + j9$
c. $\theta_i = 75°$, $\lambda = 0.1$ m, $\sigma = 0.5$, $L = 12T$, $\varepsilon = 80 + j9$

12. Comparison of Variance for Different Cell Sizes for: 20

$\theta_i = 30°$, $\lambda = 0.25$ m, $\sigma = 0.2$, $\varepsilon = 30 + j2$

13. Comparison of Variance for Different Cell Sizes for: 21

$\theta_i = 30°$, $\lambda = 0.25$ m, $\sigma = 0.5$, $\varepsilon = 30 + j2$

14. Comparison of Variance for Different Cell Sizes for: 22

$\theta_i = 75°$, $\lambda = 0.25$ m, $\sigma = 0.5$, $\varepsilon = 30 + j2$

15. Comparison of Variance for Different Cell Sizes for: 23

$\theta_i = 75°$, $\lambda = 0.1$ m, $\sigma = 0.2$, $\varepsilon = 30 + j2$

16. Mean and Variance of Scattered Power for: 24

a. $\theta_i = 30°$, $\lambda = 0.1$ m, $\sigma = 0.05$, $L = 3T$, $\varepsilon = 30 + j2$
b. $\theta_i = 30°$, $\lambda = 0.1$ m, $\sigma = 0.2$, $L = 3T$, $\varepsilon = 30 + j2$
c. $\theta_i = 30°$, $\lambda = 0.1$ m, $\sigma = 0.5$, $L = 3T$, $\varepsilon = 30 + j2$

17. Mean and Variance of Scattered Power for: 26

a. $\theta_i = 30°$, $\lambda = 0.25$ m, $\sigma = 0.2$, $L = 3T$, $\varepsilon = 30 + j2$
b. $\theta_i = 30°$, $\lambda = 0.1$ m, $\sigma = 0.2$, $L = 3T$, $\varepsilon = 30 + j2$

18. Mean and Variance of Scattered Power for: 27

a. $\theta_i = 30°$, $\lambda = 0.25$ m, $\sigma = 0.5$, $L = 3T$, $\varepsilon = 30 + j2$
b. $\theta_i = 30°$, $\lambda = 0.1$ m, $\sigma = 0.5$, $L = 3T$, $\varepsilon = 30 + j2$

19. Mean and Variance of Scattered Power for: 28

a. $\theta_i = 75°$, $\lambda = 0.25$ m, $\sigma = 0.5$, $L = 3T$, $\varepsilon = 30 + j2$
b. $\theta_i = 75°$, $\lambda = 0.1$ m, $\sigma = 0.5$, $L = 3T$, $\varepsilon = 30 + j2$

20. Mean and Variance of Scattered Power for H-pol for: 29

a. $\theta_i = 75°$, $\lambda = 0.25$ m, $\sigma = 0.5$, $L = 3T$, $\varepsilon = 30 + j2$
b. $\theta_i = 75°$, $\lambda = 0.1$ m, $\sigma = 0.5$, $L = 3T$, $\varepsilon = 30 + j2$

21. Comparison of Normalized Variance for Different Surface Roughness for $\theta_i = 75°$, $\lambda = 0.1$ m, $L = 3T$, $\varepsilon = 30 + j2$ 31

22. Comparison of Normalized Variance for Different Surface Roughness for $\theta_i = 30°$, $\lambda = 0.25$ m, $L = 3T$, $\varepsilon = 30 + j2$ 32

23. Mean and Variance of Scattered Power for: 36,37

a. $\theta_i = 30°$, $\lambda = 0.1$ m, $\sigma = 0.2$, $L = 3T$, $\varepsilon = 30 + j2$, $\psi = 0°$
b. $\theta_i = 30°$, $\lambda = 0.1$ m, $\sigma = 0.2$, $L = 3T$, $\varepsilon = 30 + j2$, $\psi = 30°$
c. $\theta_i = 30°$, $\lambda = 0.1$ m, $\sigma = 0.2$, $L = 3T$, $\varepsilon = 30 + j2$, $\psi = 45°$
d. $\theta_i = 30°$, $\lambda = 0.1$ m, $\sigma = 0.2$, $L = 3T$, $\varepsilon = 30 + j2$, $\psi = 60°$
e. $\theta_i = 30°$, $\lambda = 0.1$ m, $\sigma = 0.2$, $L = 3T$, $\varepsilon = 30 + j2$, $\psi = 90°$

24. Mean and Variance of Scattered Power for: 38,39

a. $\theta_i = 75°$, $\lambda = 0.25$ m, $\sigma = 0.5$, $L = 3T$, $\varepsilon = 30 + j2$, $\psi = 0°$
b. $\theta_i = 75°$, $\lambda = 0.25$ m, $\sigma = 0.5$, $L = 3T$, $\varepsilon = 30 + j2$, $\psi = 30°$
c. $\theta_i = 75°$, $\lambda = 0.25$ m, $\sigma = 0.5$, $L = 3T$, $\varepsilon = 30 + j2$, $\psi = 45°$
d. $\theta_i = 75°$, $\lambda = 0.25$ m, $\sigma = 0.5$, $L = 3T$, $\varepsilon = 30 + j2$, $\psi = 60°$
e. $\theta_i = 75°$, $\lambda = 0.25$ m, $\sigma = 0.5$, $L = 3T$, $\varepsilon = 30 + j2$, $\psi = 90°$

25. Mean and Variance of Scattered Power for: 40,41

a. $\theta_i = 30°$, $\lambda = 0.1$ m, $\sigma = 0.2$, $L = 3T$, $\varepsilon = 2 + j1.6$, $\psi = 0°$
b. $\theta_i = 30°$, $\lambda = 0.1$ m, $\sigma = 0.2$, $L = 3T$, $\varepsilon = 2 + j1.6$, $\psi = 30°$
c. $\theta_i = 30°$, $\lambda = 0.1$ m, $\sigma = 0.2$, $L = 3T$, $\varepsilon = 2 + j1.6$, $\psi = 50°$
d. $\theta_i = 30°$, $\lambda = 0.1$ m, $\sigma = 0.2$, $L = 3T$, $\varepsilon = 2 + j1.6$, $\psi = 70°$
e. $\theta_i = 30°$, $\lambda = 0.1$ m, $\sigma = 0.2$, $L = 3T$, $\varepsilon = 2 + j1.6$, $\psi = 90°$

Tables

1. Surface Dielectric Constants 8

2. Variance as a Function of Wavelength 25

3. Comparison of Measured σ^o with Calculated σ^o 33

4. Complex Polarization Factor 34

Analytical Characterization of Bistatic Scattering From Gaussian Distributed Surfaces

1. INTRODUCTION

Accurate statistical modeling of the clutter encountered by a radar system at a particular site is critical to the proper design of the system. Clutter is any unwanted radar echo, such as reflections from the terrain. When the clutter is as large as the expected target return, the radar assumes the return is due to a target being present, and a false alarm occurs. Clutter is, therefore, a significant factor in determining the optimum value of the minimum detectable signal, (smallest target) for the required false alarm rate.[1] The clutter returns are not equal but are distributed in magnitude. If there are more high energy returns due to clutter than a model predicts, the false alarm rate will be unacceptably high. Conversely, fewer high energy returns than expected means that the probability of detection could have been improved by lowering the detection threshold.

Also, theoretical modeling of scattering from rough surfaces that cause clutter is very important because accurate measurements of clutter are very difficult and expensive to perform, and are sometimes unreliable. The mean and variance of clutter can be determined experimentally, but this requires many measurements of similar, independent clutter cells to be made. These measured values would then only be valid for the specific geometry and type of

Received for Publication 19 November 1991

[1] Skolnik, M.I. (1980) *Introduction to Radar Systems*, McGraw-Hill Book Company, New York.

clutter being measured. Any changes in polarization, frequency, radar deployment, geometry, seasonal variation, or even moisture content of the ground will result in a completely different set of statistics. Even measurements made under identical conditions can vary by up to 10 dB.[2] For these reasons, theoretical models of clutter statistics are important. The power scattered from a rough surface is usually assumed to be Rayleigh distributed. The Rayleigh distribution function is:

$$f(x) = \frac{x^2}{\alpha^2} e^{-x/2\alpha^2} U(x). \qquad (1)$$

Figure 1 is a plot of this distribution function for several values of α. The assumption of Rayleigh distributed clutter is valid for an infinite scattering surface of many similar sized scatterers. If the scatterers differ significantly in size or if the number of scatterers is decreased by limiting the cell size, the probability density function of the scattered power will no longer have a Rayleigh distribution.

An application of this is in short pulse radars where the clutter patch is limited in the range dimension. For such radars, the requirement of a large surface with many scattering centers is violated. In this report, the statistics of the power scattered from a rough surface with a finite range dimension will be determined using a physical optics model.

The effect of polarization on rough surface scattering will also be examined. Because the reflection coefficient of a surface is polarization dependent, the statistics of the scattering will also be a function of the incident polarization. In a study by Papa and Woodworth,[3] the mean and variance of the scattered power were investigated for horizontal incident polarization. Arbitrary linear polarization states will be studied to determine the effect of polarization on the scattering statistics.

[2] Long, M.W. (1975) *Radar Reflectivity of Land and Sea*, D.C. Heath and Company, Lexington, MA.

[3] Papa, R.J., and Woodworth, M.B. (1991) *The Mean and Variance of Diffuse Scattered Power as a Function of Clutter Resolution Cell Size*, RADC-TR-91-09.

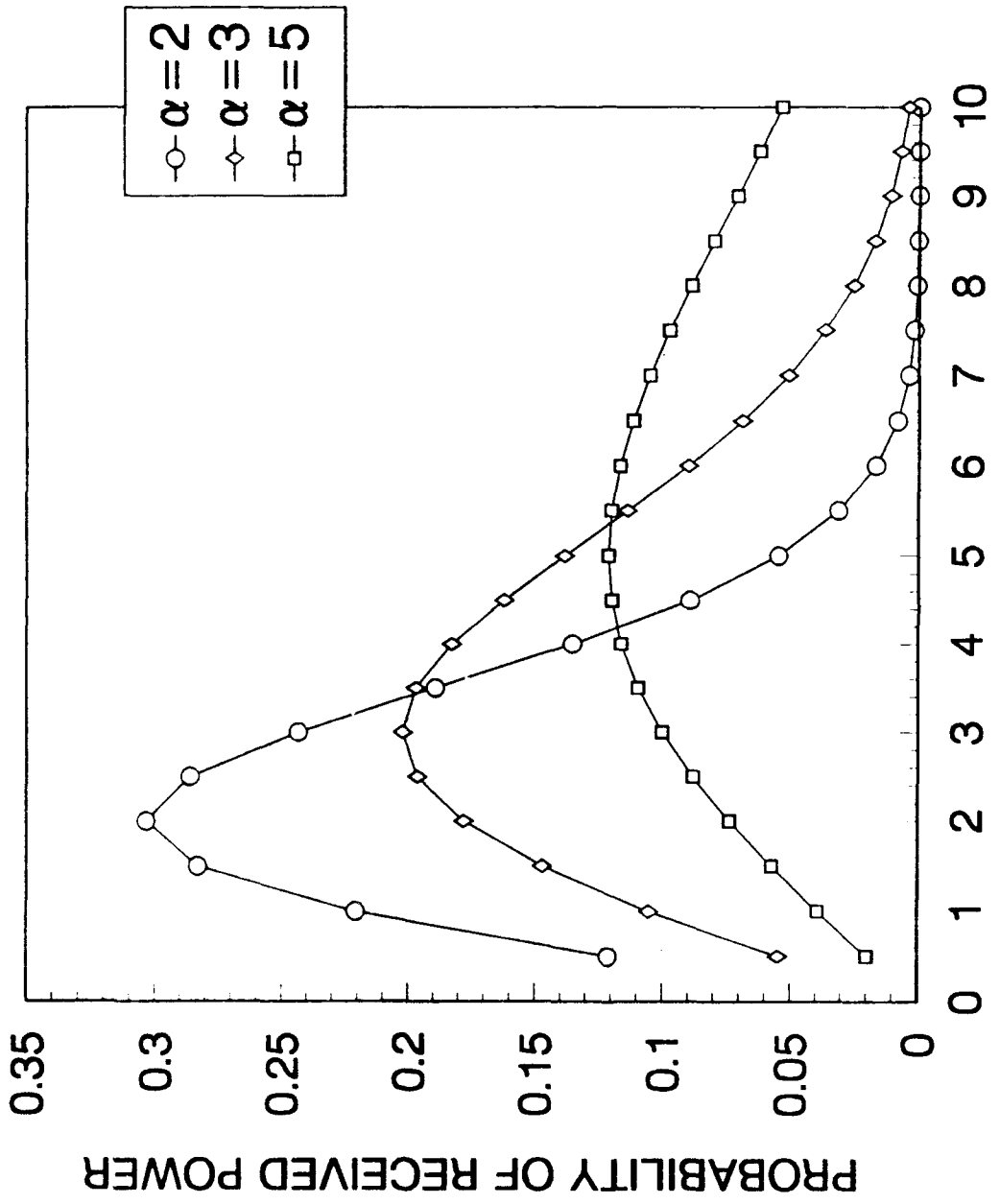

Figure 1. Rayleigh Distribution Functions

2. THEORETICAL FORMULATION

The normalized cross section of a rough surface, σ^o is

$$\sigma^o = \left(\frac{4\pi R_o^2}{A}\right)\left[< (E_s/E_i)\,(E_s/E_i)^* > - < (E_s/E_i) >^2\right] \tag{2}$$

where E_i is the incident field, E_s is the scattered field, R_o is the distance from the surface to the field point, A is the area of the illuminated cell, * indicates the complex conjugate, and the angle brackets indicate an ensemble average over the surface variables. Figure 2 depicts the scattering geometry. For a one dimensionally rough surface only in-plane scattering occurs ($\phi = 0^o$), and there is no shadowing.[4]

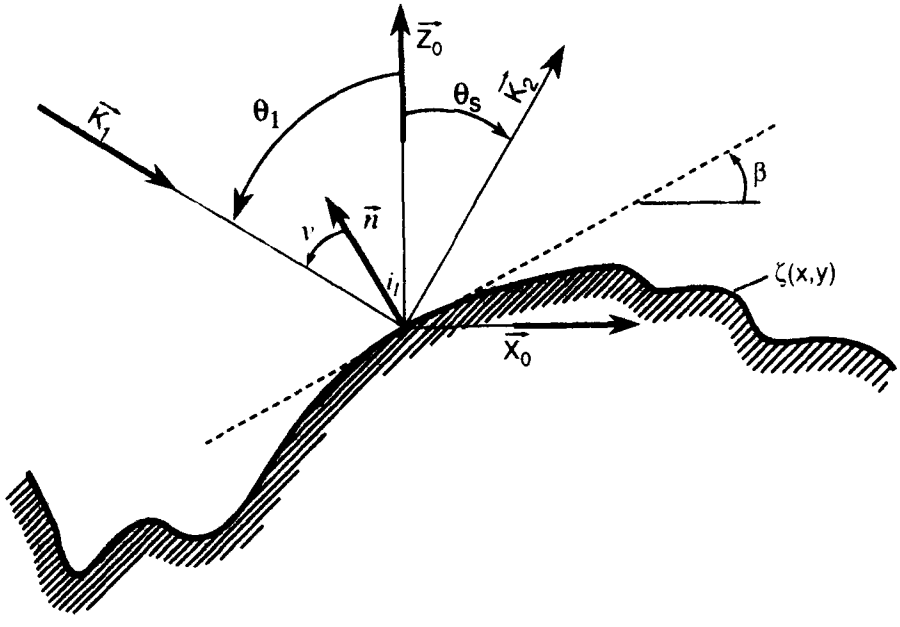

Figure 2. Scattering Geometry

[4] Beckmann, P., and Spizzichino, A. (1963) *The Scattering of Electromagnetic Waves from Rough Surfaces*, The MacMillan Co., New York.

The surface geometry is shown in Figure 3. The points x_1 and x_2 are two random points separated by the correlation distance, τ, with heights ξ_1 and ξ_2. The correlation distance defines the density of the irregularities. The local slopes of the rough surface at these points are μ_1 and μ_2. The distribution of the heights is described by a Gaussian distribution function because this is the most typical distribution of a rough surface. This distribution function is given by:

$$w(\xi) = \frac{1}{\sigma\sqrt{2\pi}} \exp\left(\frac{\xi^2}{2\sigma^2}\right) \tag{3}$$

where σ is the standard deviation of the surface heights and σ^2 is the variance of ξ. The variance can be chosen to represent the desired degree of roughness and the correlation distance chosen for the desired density of the irregularities.

For a one dimensionally rough surface used in this study, the expression for normalized mean cross section, σ^o, is:

$$\sigma^o = \left(\frac{2\pi R_o}{L}\right)\left(<|E_s/E_i|^2> - <|E_s/E_i|>^2\right). \tag{4}$$

The scattered field is a cylindrical wave calculated by evaluating the Helmholtz integral equation:

$$E_s = \int_L E\frac{\partial\psi}{\partial n} - \psi\frac{\partial E}{\partial n}\, dL \tag{5}$$

where: $\psi = \left(\frac{i}{4}\right)\sqrt{2/(\pi k_s \bullet R')}\exp\left(i k_s \bullet R'\right)$

k_s = scattered wave vector

$R' = R_o - r_o$

R_o = vector from origin to field point

r = vector from origin to source on the surface

$E = (1+R)\,E_i$ is the total field on the surface

R = Fresnel reflection coefficient

$\frac{\partial}{\partial n}$ = normal derivative on surface, S

L = range dimension of the scattering cell

and the time dependence, $\exp(-j\omega t)$, is supressed.

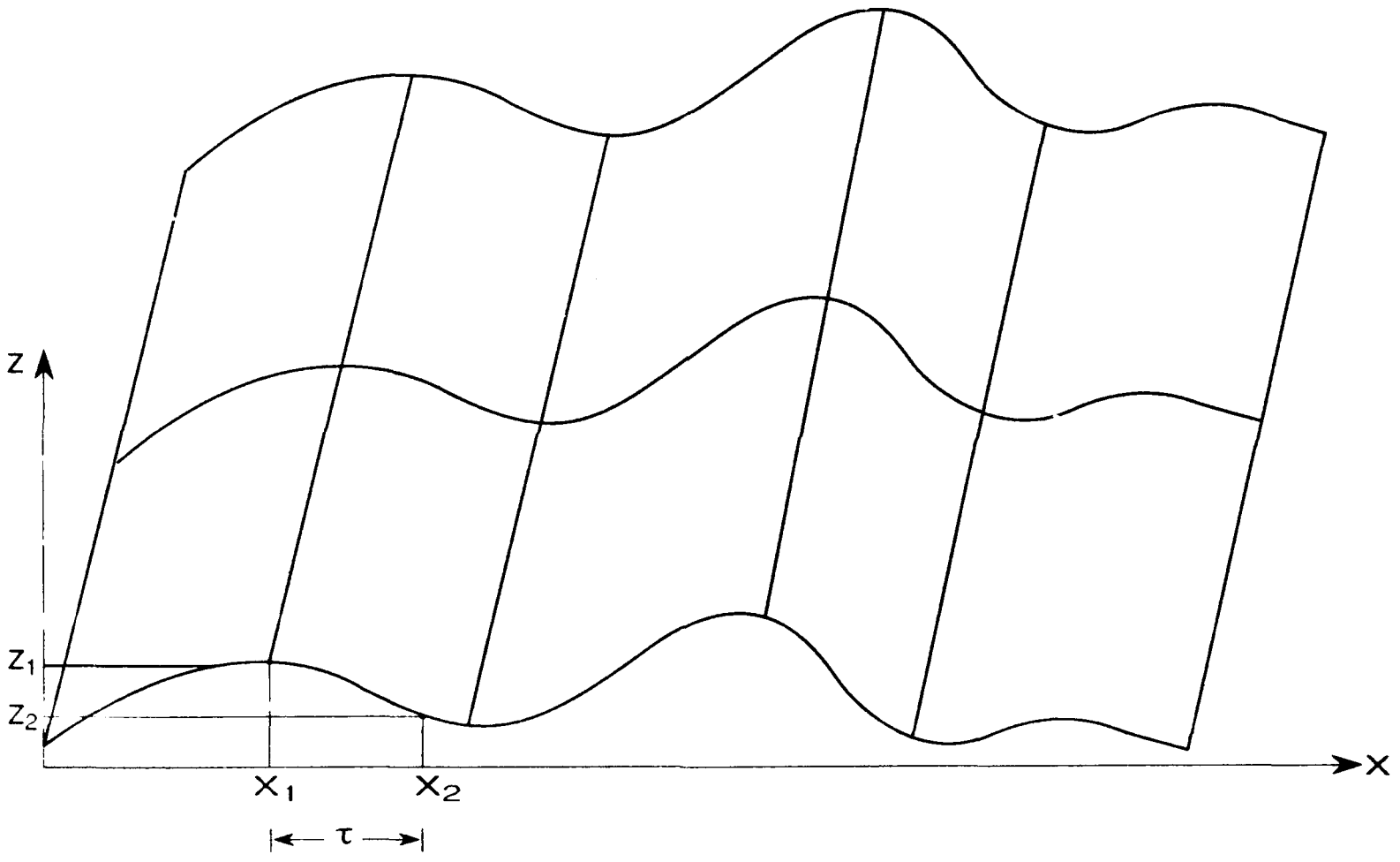

Figure 3. Surface Geometry

The most general expression for σ^o involves a six-fold integral over the surface variables, x_1, x_2, ξ_1, ξ_2, μ_1 and μ_2 . However, Papa and Woodworth show that because the surface heights are regarded as a stationary random process, the integral is a function solely of the separation between the two surface points, $\tau = x_1 - x_2$, which simplifies the six-fold integral to a five-fold integral. The five-fold integral can be further simplified to a four-fold integral because the expression for σ^o is a function of the height differences, $\xi = \xi_1 - \xi_2$. Then, by assuming that the surface slopes are small, $\sqrt{2}\ \sigma / T < 1$, the integrals over μ_1 and μ_2 can be performed analytically and the expression for σ^o can then be written as a double integral given by:

$$\sigma^o = \left[\frac{\pi F^2}{2 L \lambda}\right] \int_{-L/2}^{L/2} dx_1 \int_{-L/2}^{L/2} dx_2 \left[\chi_2 - \chi_1 \chi_1^*\right] \cos(v_x \tau) \qquad (6)$$

where: $\tau = x_1 - x_2$

$\chi_2 = \exp[-\Sigma^2 (1 - C_{12})]$ is the characteristic function for bivariate height distribution

$\chi_1 = \exp(-\Sigma^2/2)$ is the characteristic function for univariate height distribution

$C_{12} = \exp[-(x_1 - x_2)^2/T^2]$

$\Sigma^2 = \sigma^2 v_z^2$ = Rayleigh parameter squared

σ = rms surface height

$v_x = (2\pi/\lambda)(\sin(\theta_i) - \sin(\theta_s))$

$v_z = (2\pi/\lambda)(\cos(\theta_i) + \cos(\theta_s))$

$$F = \frac{2R[1 + \cos(\theta_i + \theta_s)]}{\cos\theta_i + \cos\theta_s}.$$

Note that it is the reflection coefficient in the factor F that causes σ^o to be a function of the polarization of the incident wave and the dielectric properties of the surface.

The variance of the scattered power, σ^{oo} is given by (see Papa and Woodworth):

$$\sigma^{oo} = \left(\frac{\pi F^2}{2 L \lambda}\right)^2 \int_{L/2}^{L/2} \int \int \int dx_1\, dx_2\, dx_3\, dx_4 \cos[v_x (x_1 - x_2 + x_3 - x_4)] \cdot [\chi_4 - \chi_{12}\chi_{34}] \qquad (7)$$

where: $\chi_{12} = \exp[-\Sigma^2 (1 - C_{12})]$

$\chi_{34} = \exp[-\Sigma^2 (1 - C_{34})]$

$C_{ij} = \exp[-x_i - x_j)/T^2]$

For a Rayleigh distribution, the variance is equal to the mean squared. This definition, $\sigma^{oo} = (\sigma^o)^2$ is the definition used to calculate the Rayleigh variance in this study.[4]

3. VERTICAL POLARIZATION

The analysis done by Papa, et al is limited to the case of horizontal incident polarization. To extend the analysis to include vertical and arbitrary linear incident polarization, new reflection coefficients must be calculated.

For a perfect conductor the reflection coefficient is $R_H = -1$ for horizontal polarization, (electric vector perpendicular to the plane of incidence) and $R_V = +1$ for vertical polarization, (electric vector in the plane of incidence). Because the reflection coefficient is squared in calculating the scattered power, the results for horizontal polarization and vertical polarization are identical for a perfect conductor and will not be repeated here.

Many surfaces, however, have a complex dielectric constant, and will therefore have different reflection coefficients for vertical and horizontal polarization. A complex dielectric constant is expressed as $\varepsilon = \varepsilon' + j\varepsilon''$, where ε' is the capacivity of the medium and ε'' is the dielectric loss factor. For a good dielectric the term ε' will remain fairly constant over all radio frequencies and ε'' will be small. The relative dielectric constant is defined as $\varepsilon_r = \varepsilon/\varepsilon_o$ where ε_o is the capacivity of vacuum. Table 1 shows the relative complex dielectric constants for the surfaces which are used in this study as well as the dielectric constant for glass, which is considered to be a good dielectric.

Table 1. Surface Dielectric Constants

Surface	ε'	ε''
Moist Ground	30	2
Sea Water	80	9
Dry Sandy Loam	2	1.6
Glass	5.25	0.0115

The Fresnel reflection coefficient for horizontal polarization is given by:[5]

$$R_H = \frac{\cos\theta - \sqrt{\varepsilon_r - \sin^2\theta}}{\cos\theta + \sqrt{\varepsilon_r - \sin^2\theta}} \tag{8}$$

where θ is the local angle of incidence. The magnitude and phase of R_H are shown in Figure 4. Results for this case given by Papa, et al will be used for comparison with results obtained for vertical polarization.

For vertical polarization the reflection coefficient is:

$$R_v = \frac{\varepsilon_r \cos\theta - \sqrt{\varepsilon_r - \sin^2\theta}}{\varepsilon_r \cos\theta + \sqrt{\varepsilon_r - \sin^2\theta}} \tag{9}$$

Figure 5 shows the magnitude and phase of R_v for the dielectric constants used.

In comparing the horizontal and vertical reflection coefficients, important differences can be seen. The magnitude of the vertical reflection coefficient has a minimum value for a particular angle of incidence. This angle is called the Brewster angle and is defined as $\theta_B = \tan^{-1}\sqrt{\varepsilon_r}$. Also, the magnitude of the vertical coefficient is always less than that of the horizontal, except at normal incidence where they are equal. The differences in the reflection coefficients will have a direct effect on the scattering from a surface.

---

[5] Ruck, G.T., Barrick, D.E., Stuart, W.D., and Krichbaum, C.K. (1970) *Radar Cross Section Handbook*, Vol. 2, Plenum Press, New York.

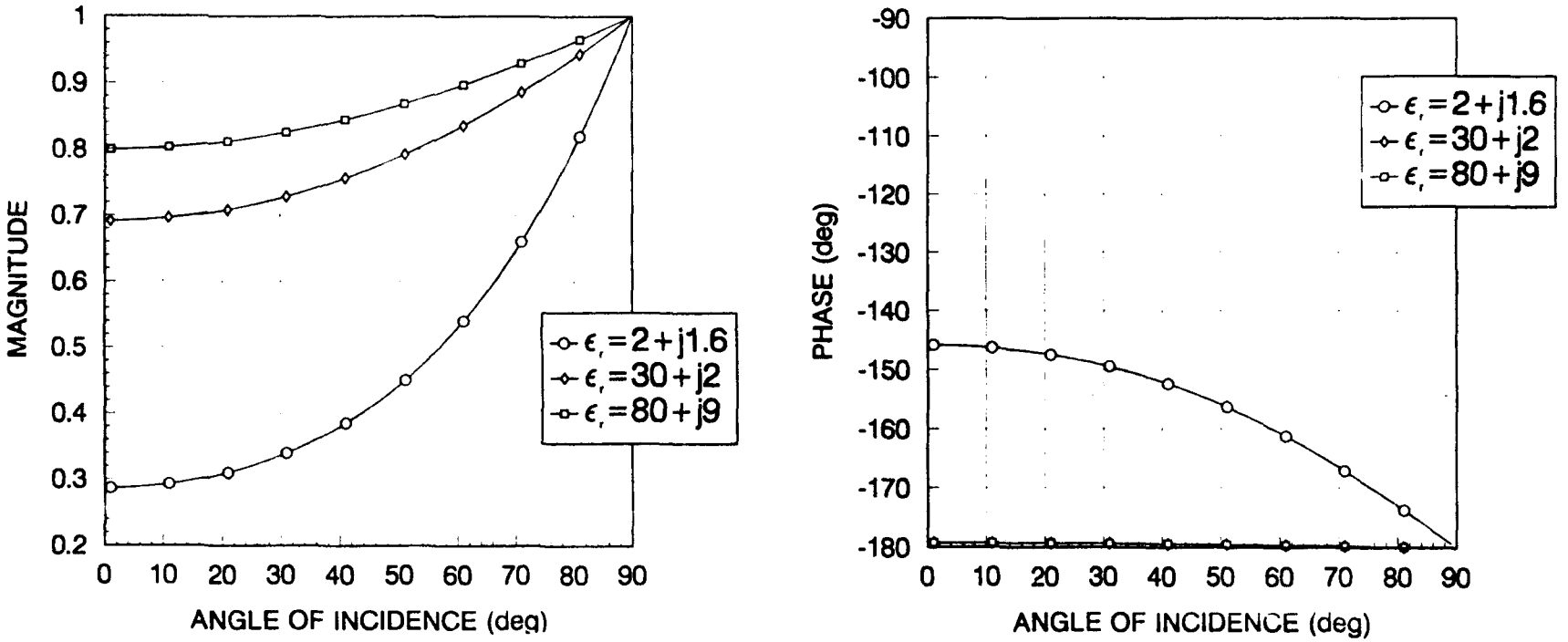

Figure 4. a. Magnitudes of Horizontal Reflection Coefficients
b. Phases of Horizontal Reflection Coefficients

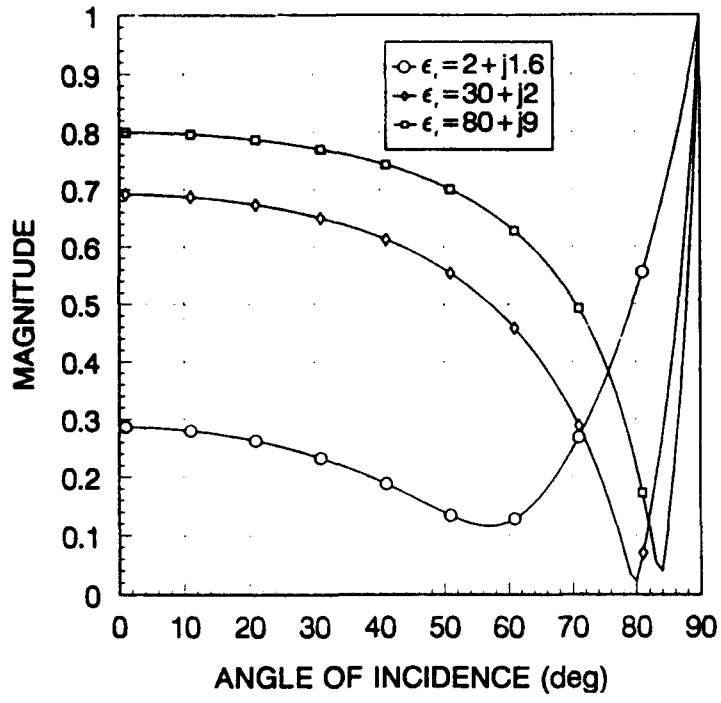

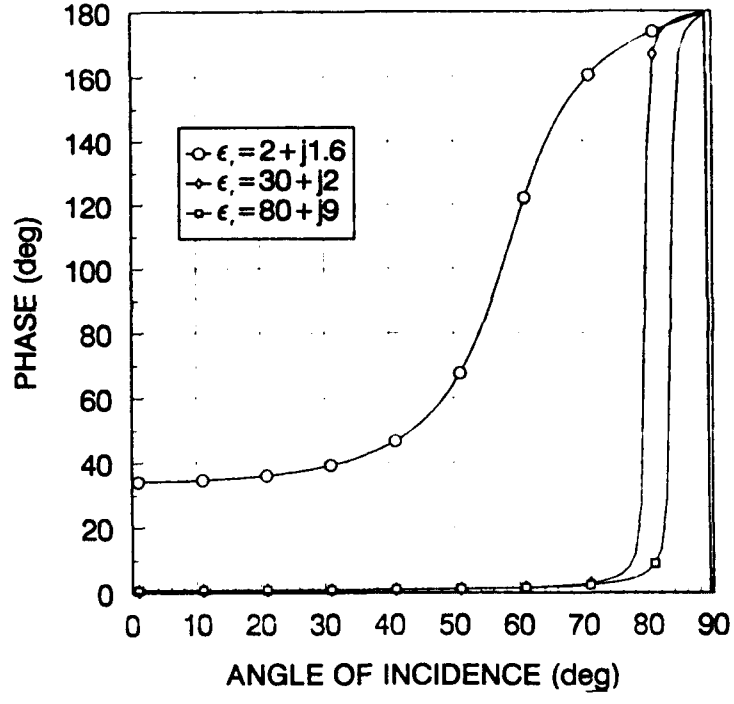

Figure 5. a. Magnitudes of Vertical Reflection Coefficients
b. Phases of Vertical Reflection Coefficients

Many of the other results, though, are valid for both horizontal and vertical polarization. Some of the other aspects that are considered are the statistical dependence of the scattering on the angle of incidence θ_i, the wavelength λ, the length of the clutter cell L, and the standard deviation in the surface heights σ. The surface roughness is defined as σ/T and $\sqrt{2}\sigma/T$ is the rms surface slope. T is the correlation length and is set to one meter for this study.

There are two factors that cause the variance of the scattered power to deviate from Rayleigh; the number of scatterers and the roughness of the surface. The number of scatterers is a function of cell size, incident angle, and the slopes of the rough surface. The roughness of the surface depends on the frequency of the incident wave as well as the surface parameters. How these parameters affect the statistics of the scattered field will be examined.

One condition necessary for Rayleigh scattering is that the illuminated area, or clutter cell, be very large with respect to the correlation distance, so that it will contain a large number of independent, nearly equal, homogeneously distributed scatterers. Decreasing the size of the clutter cell will decrease the number of scatterers and should then cause the distribution of σ^{oo} to deviate from Rayleigh. When there are only a few independent scatterers in a particular cell, their relative positions or the presence or absence of one of the scatterers causes a significant change in the reflected signal from one sample of the surface to another, resulting in a large variance.

In Figures 6 through 10, several cases are shown and the effect of changing the cell size is examined. The scattered power is normalized to both the incident field and the illuminated area, and is plotted as a function of the scattering angle. Each plot shows three curves. The curve consisting of long dashes represents the normalized mean of the scattered power, which is equivalent to the mean cross section. The normalized variance of the scattered power of a Rayleigh distributed scattering process is the curve of small dashes. The third curve with the crosses is the calculated normalized variance of the scattered power for the parameters shown.

Figure 6 is for $\theta_i = 30°$, $\lambda = 0.25$ m, $\sigma = 0.2$ m, $\varepsilon_r = 30 + j2$ with L increasing from L = 3T (Figure 6a) to L = 6T (Figure 6b) and finally L = 12T (Figure 6c). These parameters correspond to a relatively smooth patch of moist ground. Figure 7 is similar to Figure 6 but represents a rougher surface. Figures 8 and 9 are for a rough surface with a 75° angle of incidence, for vertical polarization and horizontal polarization, respectively. The effect of the different reflection coefficients is noticeable when comparing these two figures, particularly at the location of the Brewster angle, $\theta_B = 85°$. In Figure 10, $\theta_i = 75°$, $\lambda = 0.1$ m and $\sigma = 0.2$ m corresponding to a relatively smooth surface. Figure 11 represents a fairly rough water surface, $\varepsilon_r = 80 + j9$.

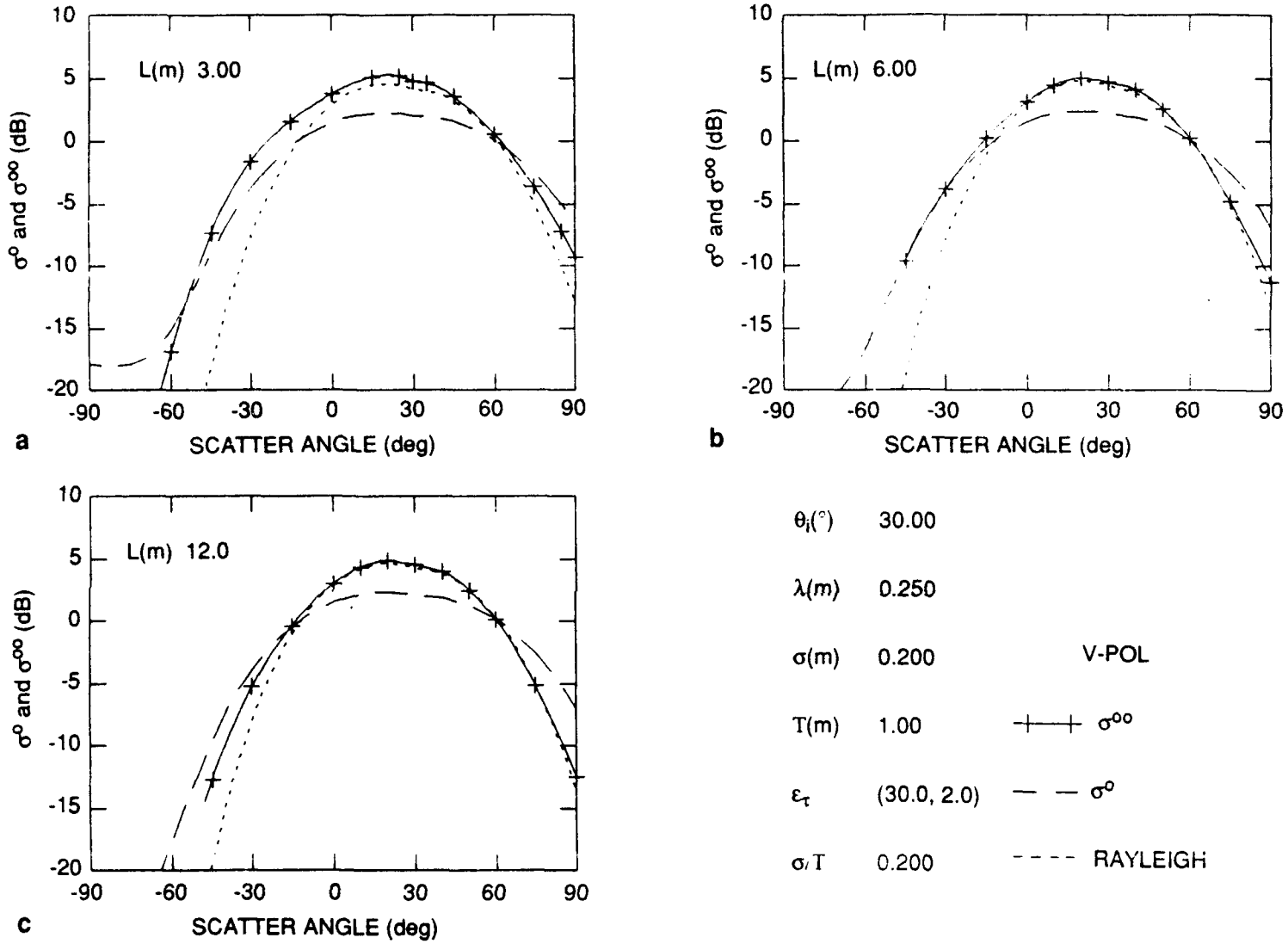

Figure 6. Mean and Variance of Scattered Power for:
a. $\theta_i = 30°$, $\lambda = 0.25$ m, $\sigma = 0.2$, $L = 3T$, $\varepsilon = 30 + j2$
b. $\theta_i = 30°$, $\lambda = 0.25$ m, $\sigma = 0.2$, $L = 6T$, $\varepsilon = 30 + j2$
c. $\theta_i = 30°$, $\lambda = 0.25$ m, $\sigma = 0.2$, $L = 12T$, $\varepsilon = 30 + j2$

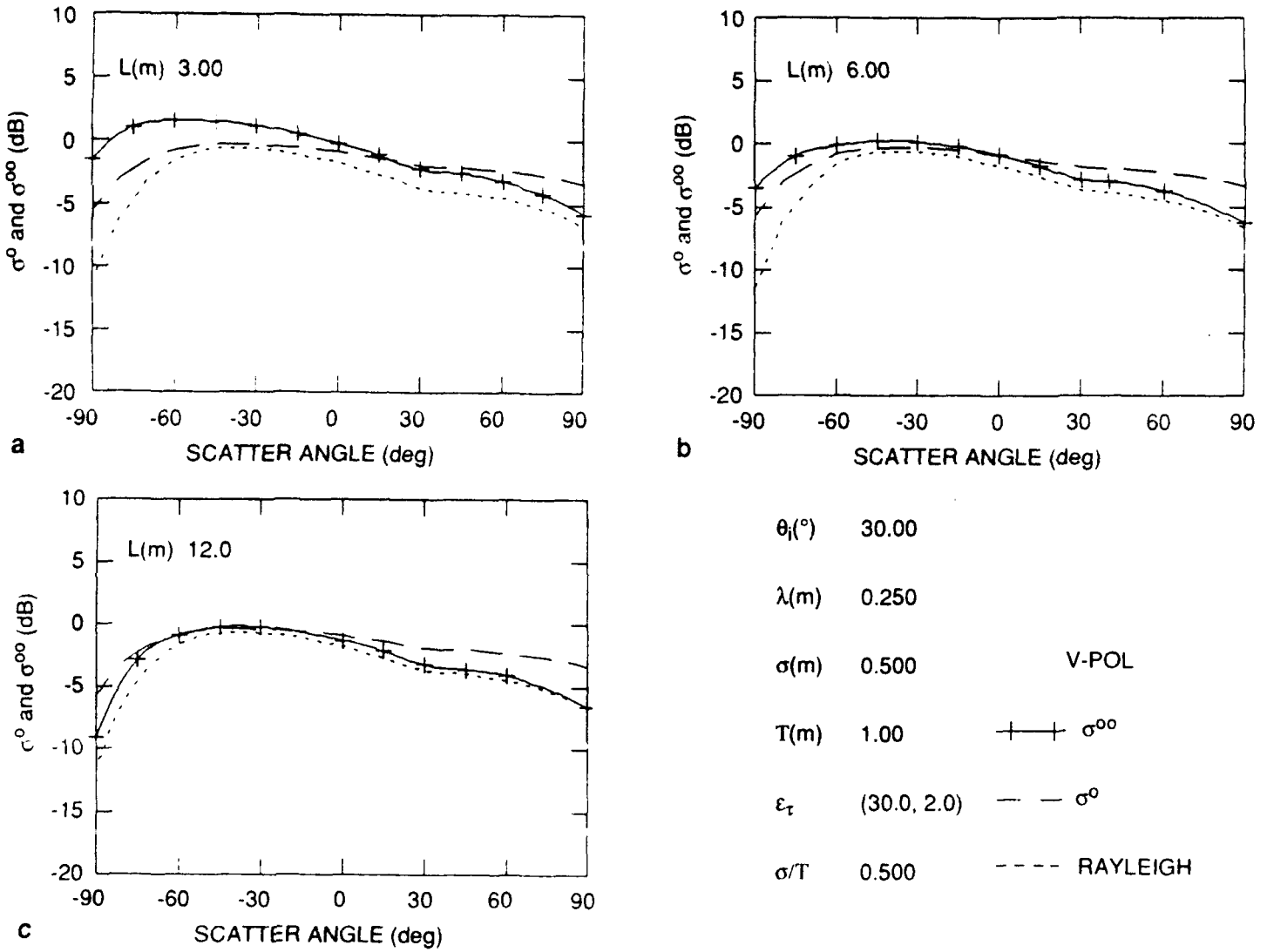

Figure 7. Mean and Variance of Scattered Power for:
a. $\theta_i = 30°$, $\lambda = 0.25$ m, $\sigma = 0.5$, $L = 3T$, $\varepsilon = 30 + j2$
b. $\theta_i = 30°$, $\lambda = 0.25$ m, $\sigma = 0.5$, $L = 6T$, $\varepsilon = 30 + j2$
c. $\theta_i = 30°$, $\lambda = 0.25$ m, $\sigma = 0.5$, $L = 12T$, $\varepsilon = 30 + j2$

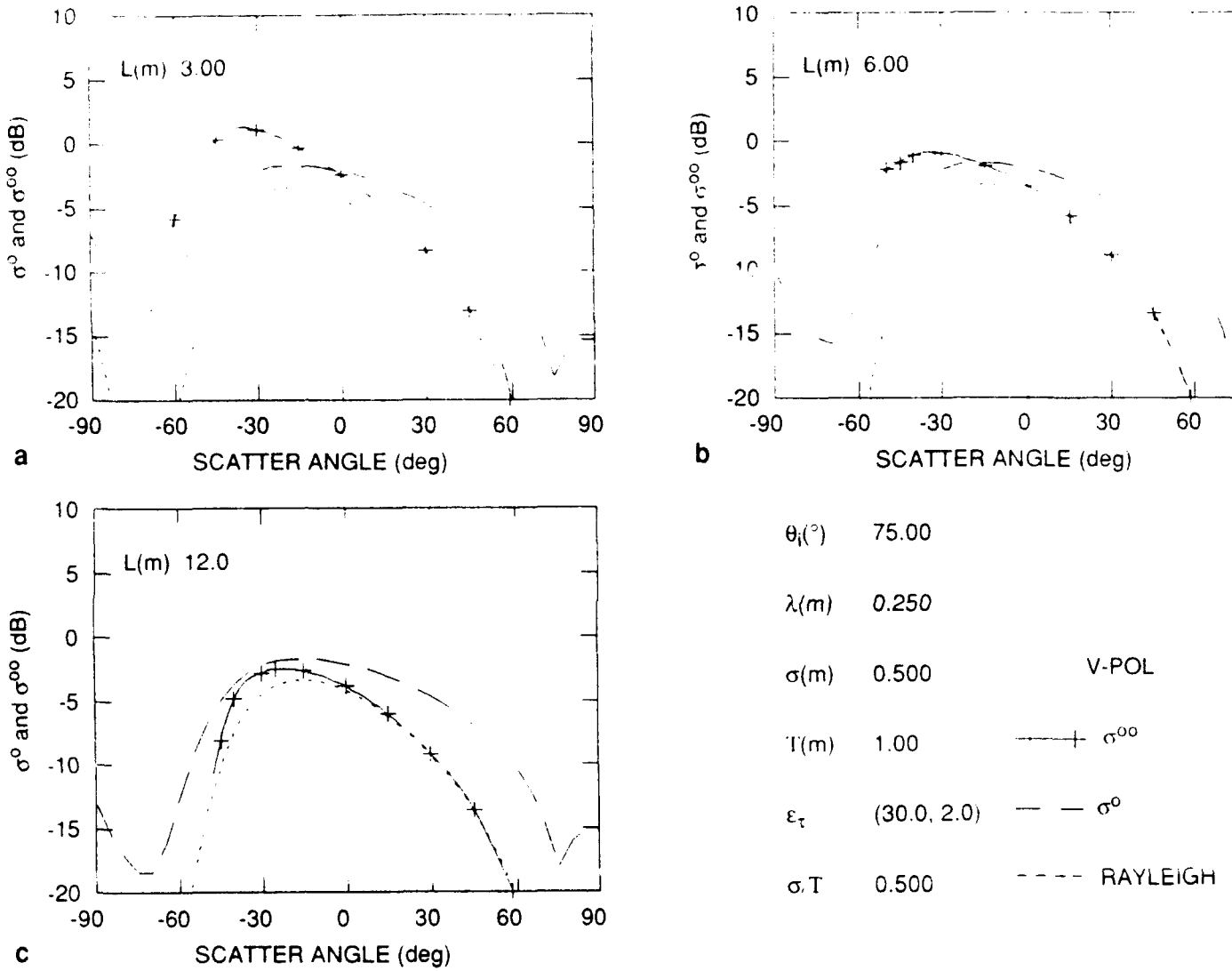

Figure 8. Mean and Variance of Scattered Power for:
a. $\theta_i = 75°$, $\lambda = 0.25$ m, $\sigma = 0.5$, $L = 3T$, $\varepsilon = 30 + j2$
b. $\theta_i = 75°$, $\lambda = 0.25$ m, $\sigma = 0.5$, $L = 6T$, $\varepsilon = 30 + j2$
c. $\theta_i = 75°$, $\lambda = 0.25$ m, $\sigma = 0.5$, $L = 12T$, $\varepsilon = 30 + j2$

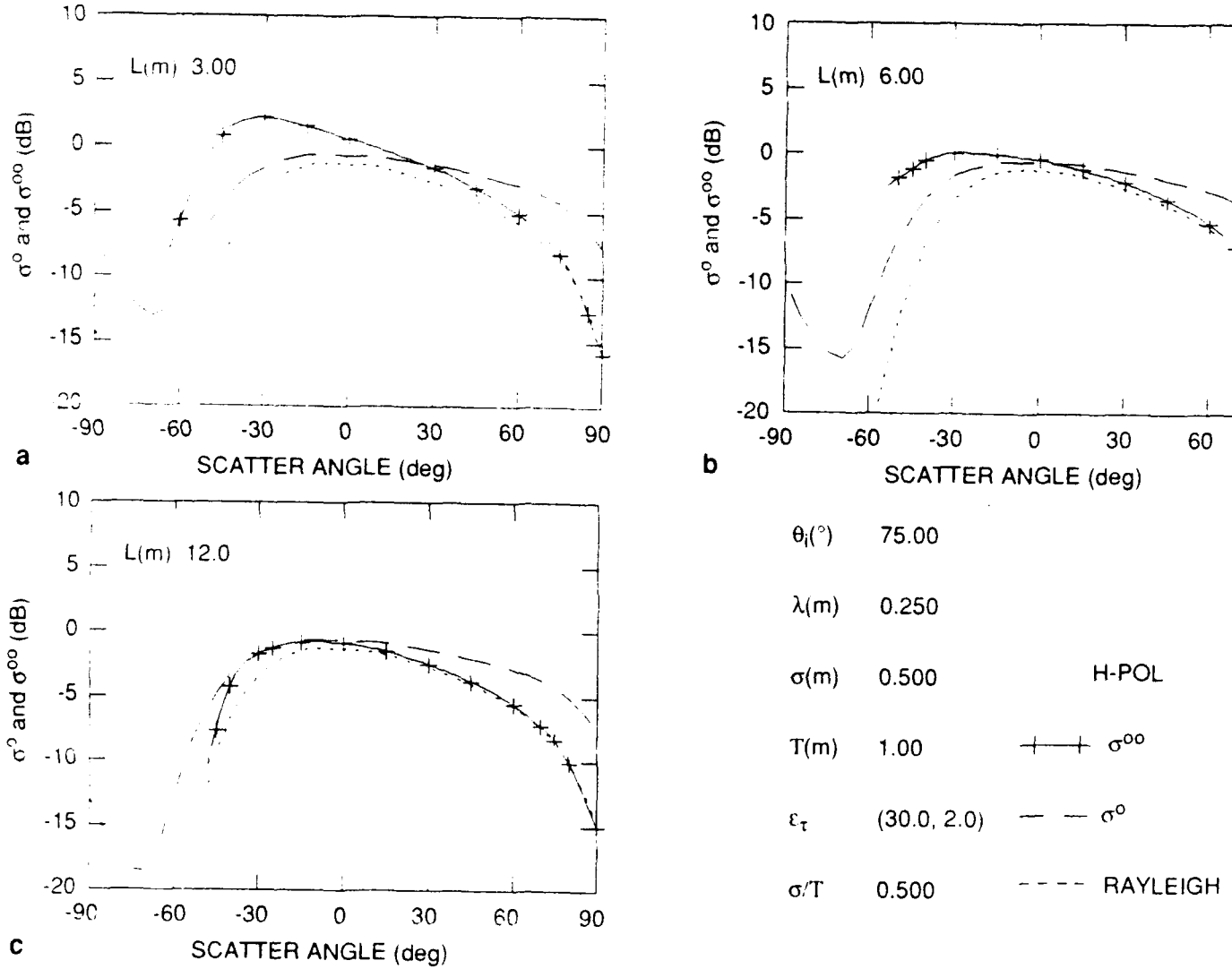

Figure 9. Mean and Variance of Scattered Power for H-pol for:
a. $\theta_i = 75°$, $\lambda = 0.25$ m, $\sigma = 0.5$, $L = 3T$, $\varepsilon = 30 + j2$
b. $\theta_i = 75°$, $\lambda = 0.25$ m, $\sigma = 0.5$, $L = 6T$, $\varepsilon = 30 + j2$
c. $\theta_i = 75°$, $\lambda = 0.25$ m, $\sigma = 0.5$, $L = 12T$, $\varepsilon = 30 + j2$

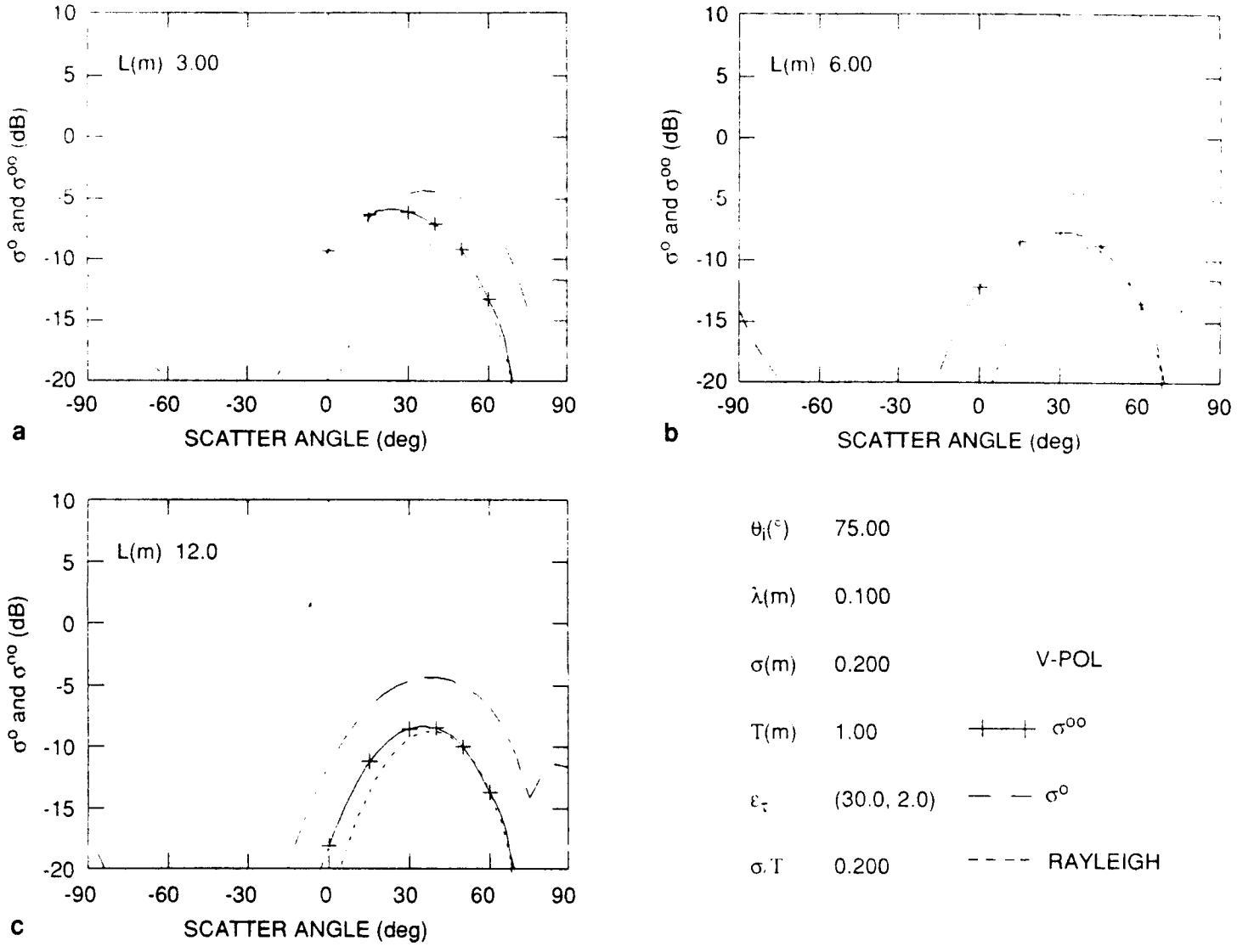

Figure 10. Mean and Variance of Scattered Power for:

a. $\theta_i = 75°$, $\lambda = 0.1$ m, $\sigma = 0.2$, $L = 3T$, $\varepsilon = 30 + j2$

b. $\theta_i = 75°$, $\lambda = 0.1$ m, $\sigma = 0.2$, $L = 6T$, $\varepsilon = 30 + j2$

c. $\theta_i = 75°$, $\lambda = 0.1$ m, $\sigma = 0.2$, $L = 12T$, $\varepsilon = 30 + j2$

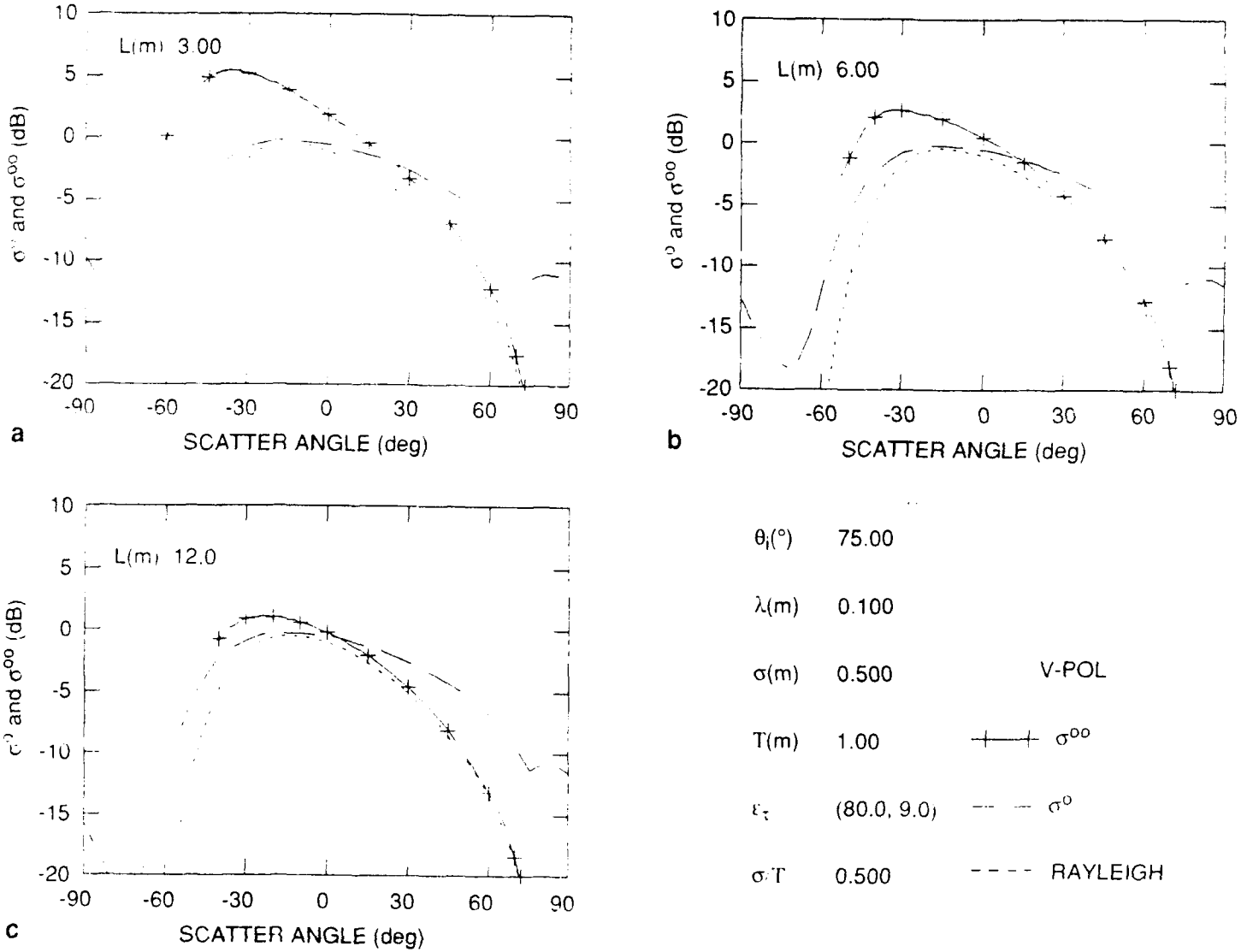

Figure 11. Mean and Variance of Scattered Power for:

a. $\theta_i = 75°$, $\lambda = 0.1$ m, $\sigma = 0.5$, $L = 3T$, $\varepsilon = 80 + j9$

b. $\theta_i = 75°$, $\lambda = 0.1$ m, $\sigma = 0.5$, $L = 6T$, $\varepsilon = 80 + j9$

c. $\theta_i = 75°$, $\lambda = 0.1$ m, $\sigma = 0.5$, $L = 12T$, $\varepsilon = 80 + j9$

In all cases, it is seen that for the smaller cell size, L = 3T, the scattering is more non-Rayleigh than for the larger clutter cells, L = 6T and L = 12T, in the scattering regions where differences in the variance can be seen. The variance of the scattered power is consistently higher for the smaller clutter cells than it is for a surface that gives rise to Rayleigh scattering.

Figures 12 through 15 show a comparison of the variance for the different cell sizes normalized to the Rayleigh value so that a value of one means the calculated value of the variance is equal to the Rayleigh value. The higher variance causes difficulties in radar design because for a constant mean value of clutter power, a larger variance corresponds to more frequent large clutter returns. This is a significant result that must be considered in the design of a short pulse radar system.

A noticeable trend seen in all of these plots is that the deviation from Rayleigh scattering becomes more severe as θ_s approaches the backscatter region, particularly when the angle of incidence is 75°. Since scattering facets must have steep slopes to cause backscatter, especially for θ_i =75°, and the distribution of the slopes is the derivative of the height distribution, and therefore also Gaussian,[6] there will be relatively few facets oriented properly to cause backscatter. Once again, the effect of having a small number of scatterers is to increase the variance of the scattered power, causing the scattering to become more non-Rayleigh.

The second factor that affects the distribution of the scattered power is the surface roughness. A wave that is incident on a rough surface will scatter in many directions and it is the relative heights and slopes of the scattering surfaces that will determine the angular distribution.

For a very smooth surface, the incident wave will be almost entirely reflected in the specular direction defined by Snell's Law. As the surface roughness increases, the scattering will become more diffusely distributed over the entire angular space.[4] Figure 16a shows the scattering for a very smooth surface, $\sigma/T = 0.05$. It is quite clear that the majority of the scattered power is in a small region around the specular direction. In Figure 16b, $\sigma = 0.2$ m corresponding to a relatively smooth surface, and the peak of the scattering in the specular direction is no longer well defined. Figure 16c is for a rougher surface with $\sigma = 0.5$ m. In this case the scattering is quite uniform over the entire region with no discernable peak in the specular region.

---

[6] Papoulis, A. (1965) *Probability, Random Variables, and Stochastic Processes*, McGraw-Hill Book Company, New York.

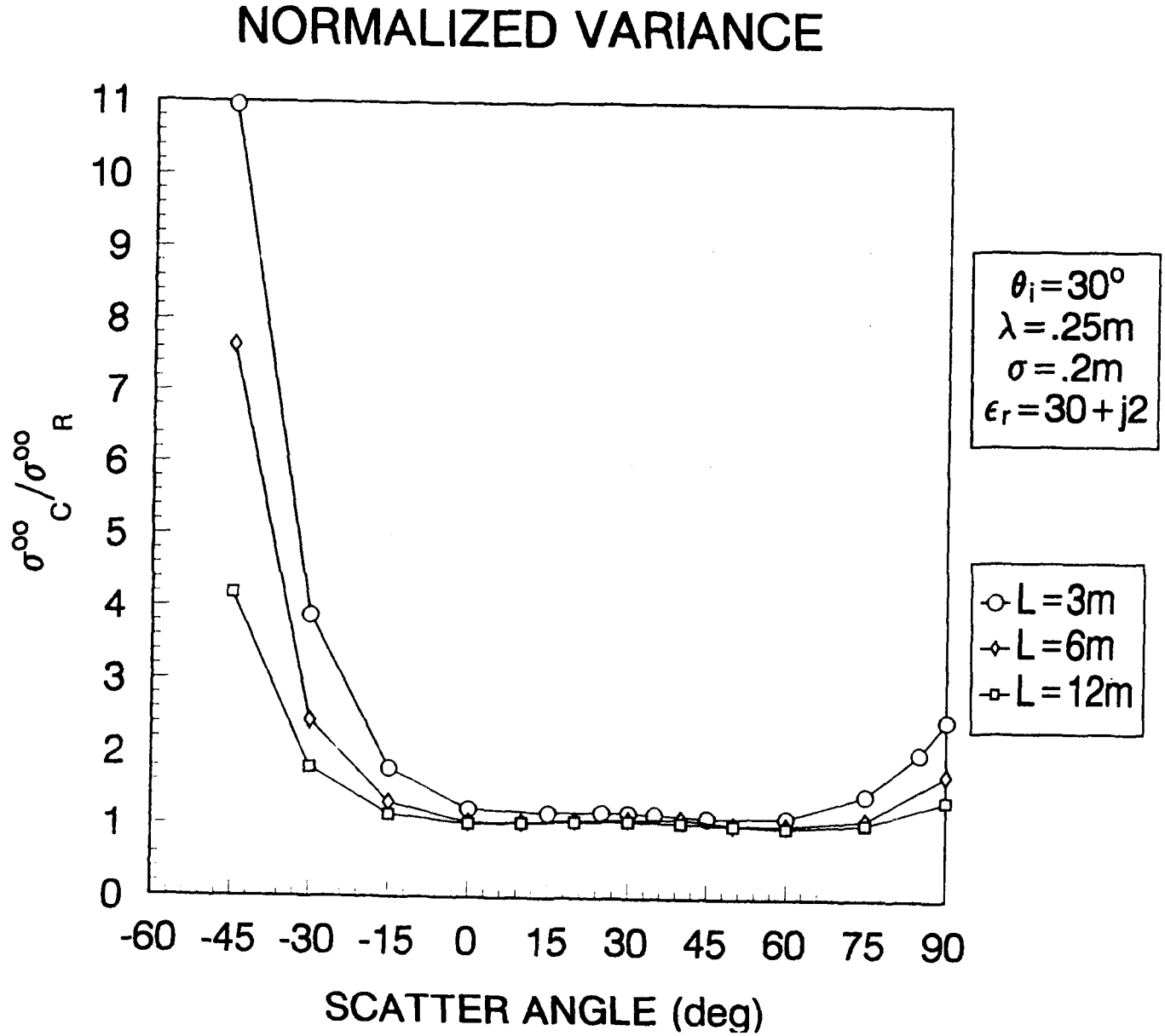

Figure 12. Comparison of Variance for Different Cell Sizes for: $\theta_i = 30^c$, $\lambda = 0.25$ m, $\sigma = 0.2$, $\varepsilon = 30 + j2$

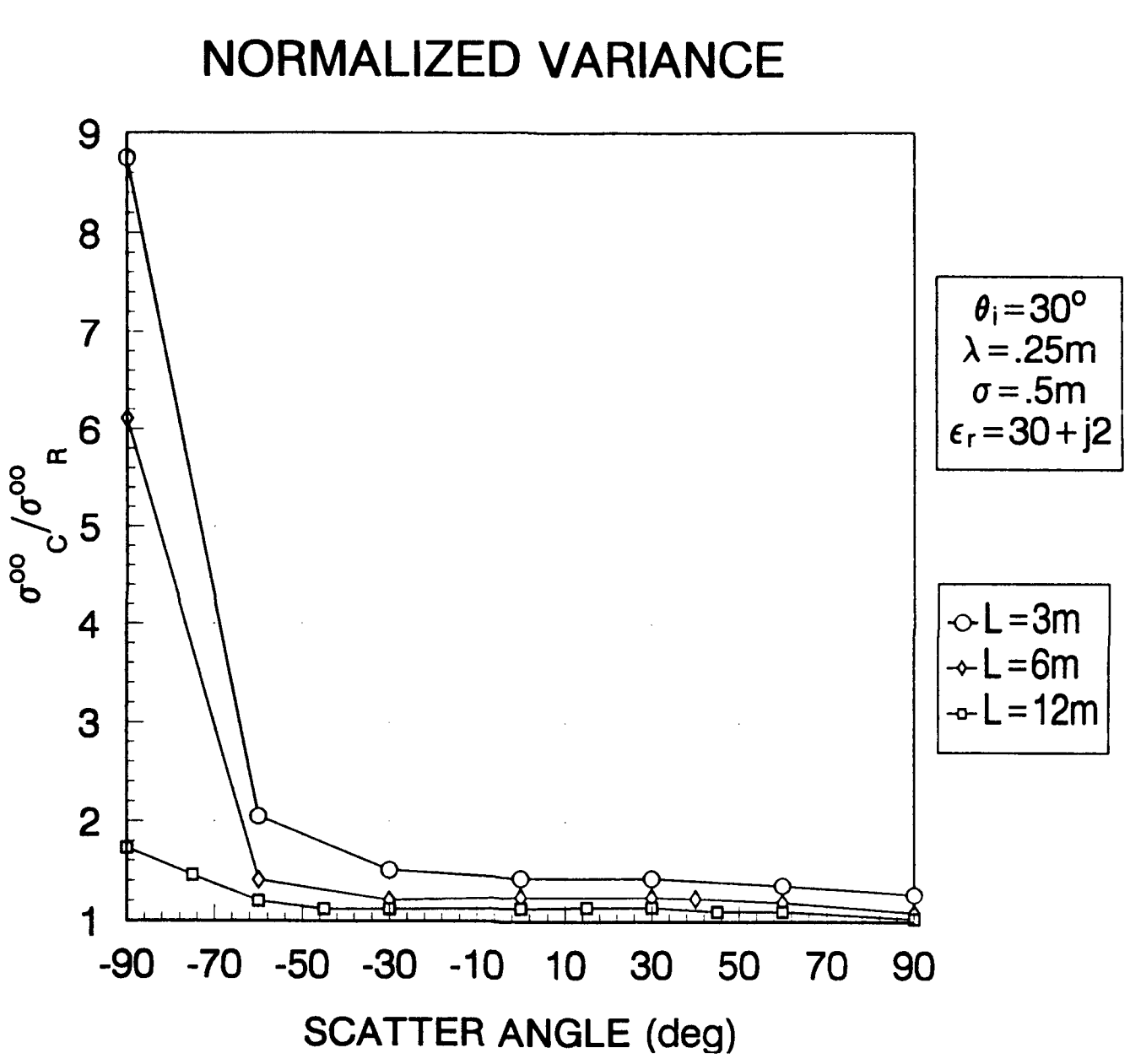

Figure 13. Comparison of Variance for Different Cell Sizes for: $\theta_i = 30°$, $\lambda = 0.25$ m, $\sigma = 0.5$, $\varepsilon = 30 + j2$

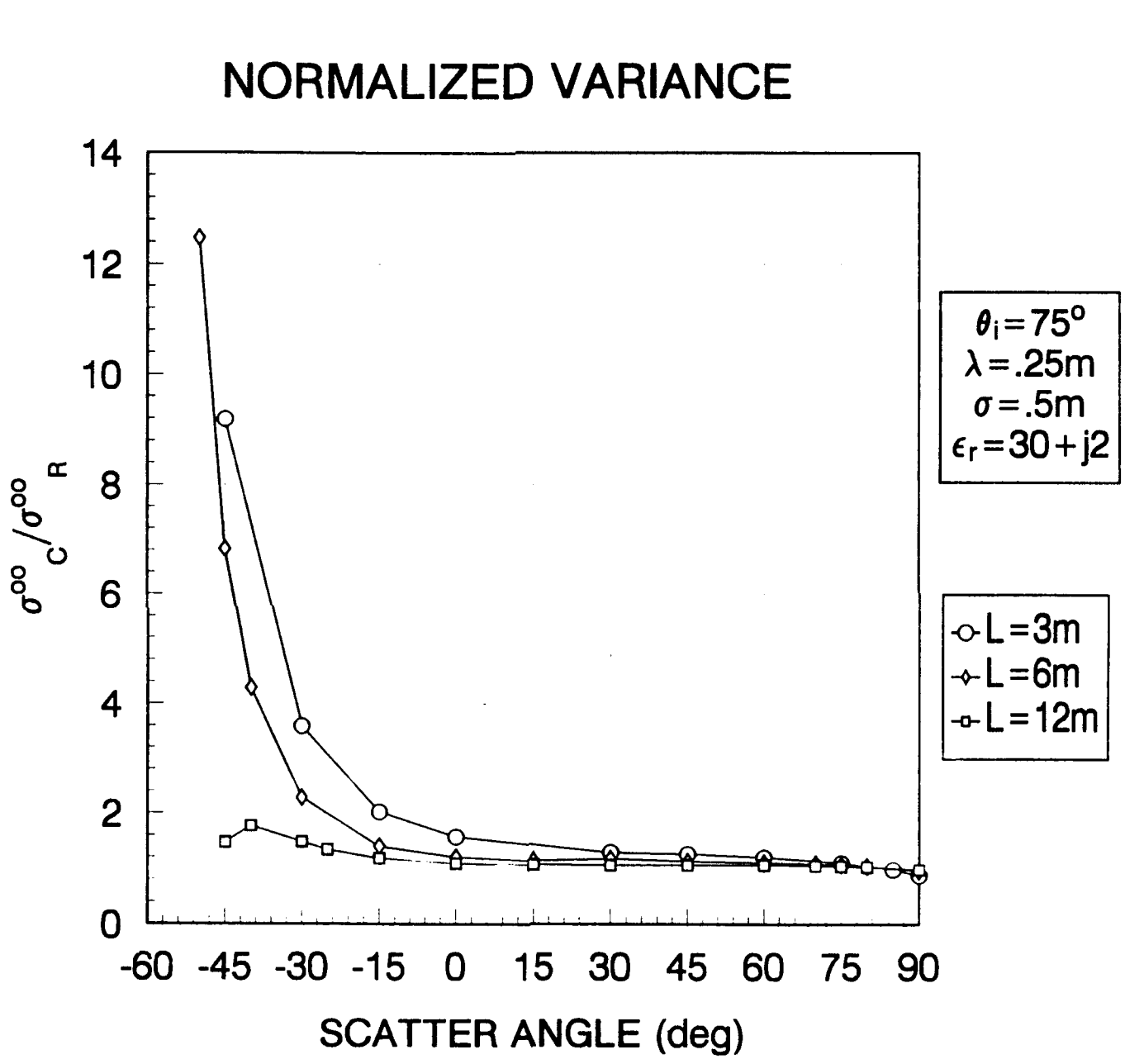

Figure 14. Comparison of Variance for Different Cell Sizes for:
$\theta_i = 75°$, $\lambda = 0.25$ m, $\sigma = 0.5$, $\varepsilon = 30 + j2$

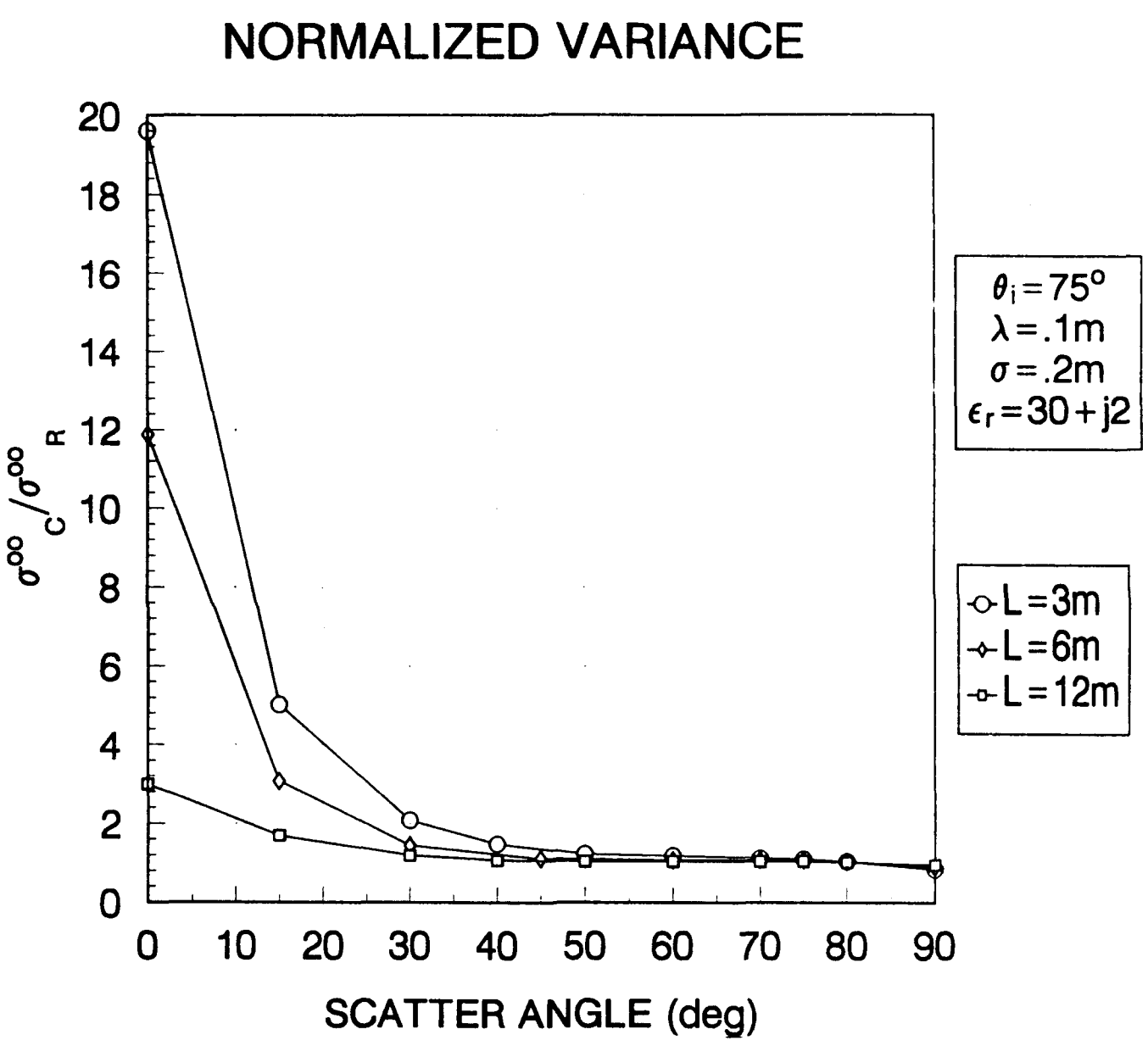

Figure 15. Comparison of Variance for Different Cell Sizes for:
$\theta_i = 75°$, $\lambda = 0.1$ m, $\sigma = 0.2$, $\epsilon = 30 + j2$

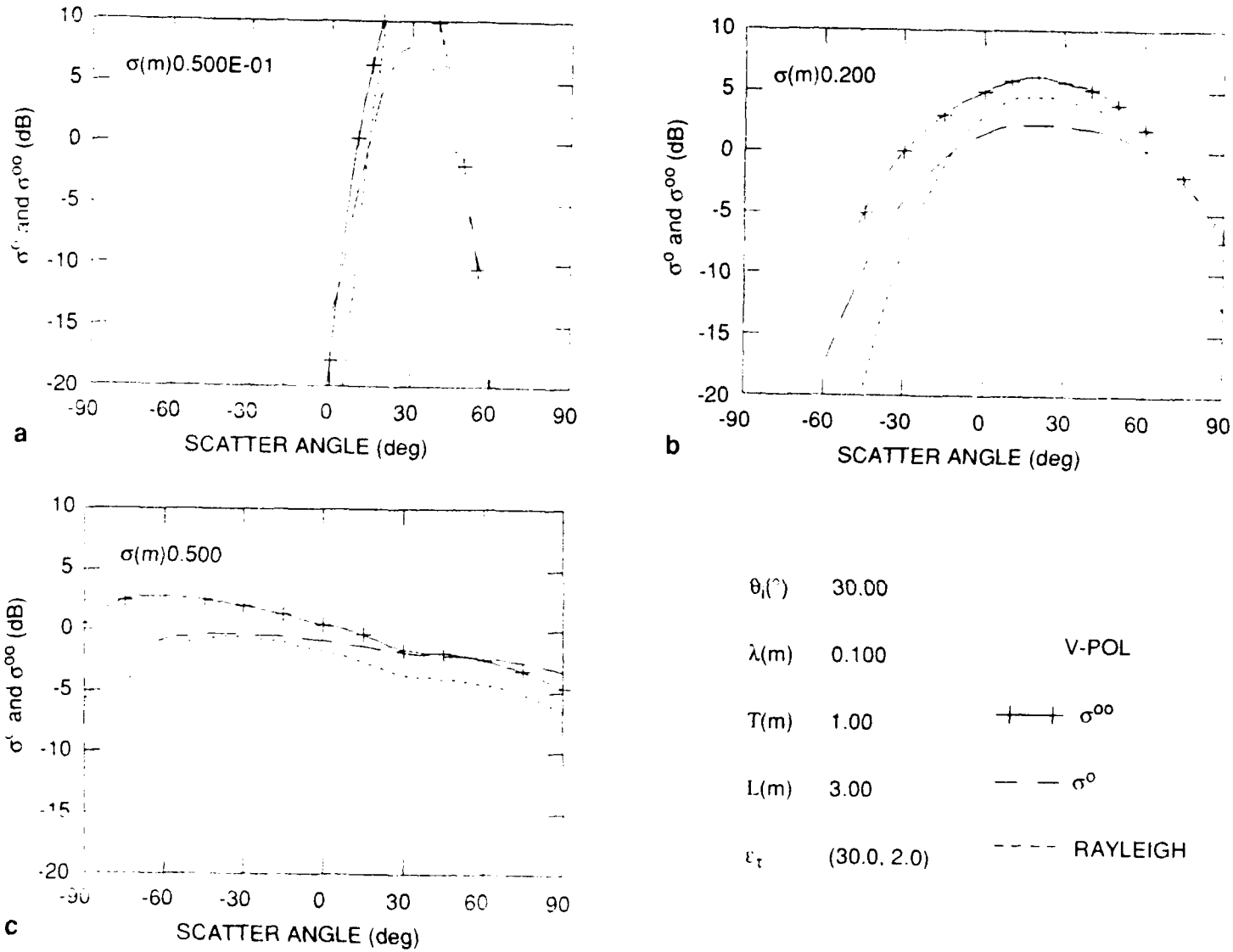

Figure 16. Mean and Variance of Scattered Power for:

a. $\theta_i = 30^o$, $\lambda = 0.1$ m, $\sigma = 0.05$, $L = 3T$, $\varepsilon = 30 + j2$

b. $\theta_i = 30^o$, $\lambda = 0.1$ m, $\sigma = 0.2$, $L = 3T$, $\varepsilon = 30 + j2$

c. $\theta_i = 30^o$, $\lambda = 0.1$ m, $\sigma = 0.5$, $L = 3T$, $\varepsilon = 30 + j2$

The relative roughness of a surface is a function of the wavelength of the incident wave so that the frequency of the incident wave will also affect the statistical distribution of the scattered power. Decreasing the wavelength increases the Rayleigh roughness parameter Σ, so that the relative heights of the scatterers is increased. Figures 17 through 20 show comparisons for cases where only the wavelength is changed.

In Figure 17, the statistics are for $\theta_i = 30°$, $\sigma = 0.2$, and $L = 3T$. Figure 17a is for the longer wavelength, $\lambda = 0.25$ m while in 17b, $\lambda = 0.1$ m. Figure 18 is similar to Figure 17 but for a rougher surface, and in Figure 19 the angle of incidence is increased to 75°. Figure 20 is the same as Figure 19 but for horizontal polarization. In all cases, the variance of the scattered power is seen to be closer to Rayleigh when the incident field has a wavelength of 0.25 m. For the shorter wavelength, or higher frequency, the scattering becomes less Rayleigh. Table 2 shows the variance of the scattered field for several wavelengths normalized to the Rayleigh value for $\theta_i = 30°$, $\sigma = 0.2$, $L = 3T$, $\theta_s = 0°$, and $\varepsilon_r = 30 + j2$. Over the range of wavelengths tested, the scattering becomes less Rayleigh as the wavelength decreases, or the roughness parameter of the surface increases.

Table 2. Variance as a Function of Wavelength.

λ (m)	σ_R^{oo} (dB)	σ_C^{oo} (dB)	$\sigma_C^{oo} / \sigma_R^{oo}$
.25	2.891	3.772	1.22
.15	2.939	4.526	1.44
.10	2.999	5.038	1.60
.05	2.987	5.614	1.83

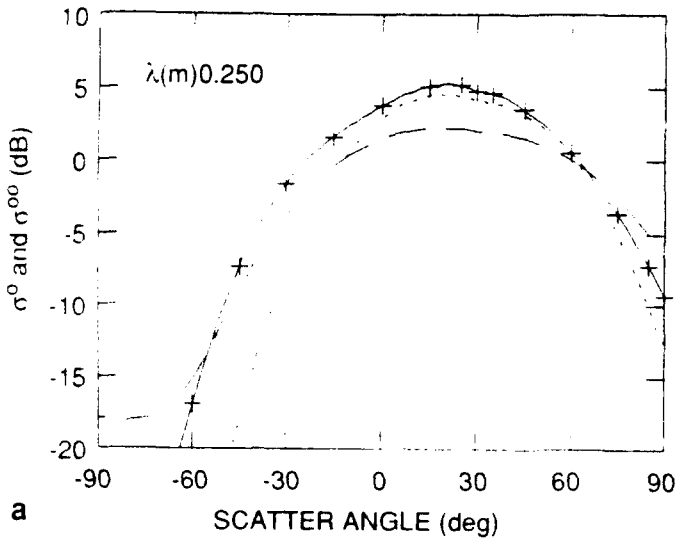

Figure 17. Mean and Variance of Scattered Power for:
a. $\theta_i = 30°$, $\lambda = 0.25$ m, $\sigma = 0.2$, $L = 3T$, $\varepsilon = 30 + j2$
b. $\theta_i = 30°$, $\lambda = 0.1$ m, $\sigma = 0.2$, $L = 3T$, $\varepsilon = 30 + j2$

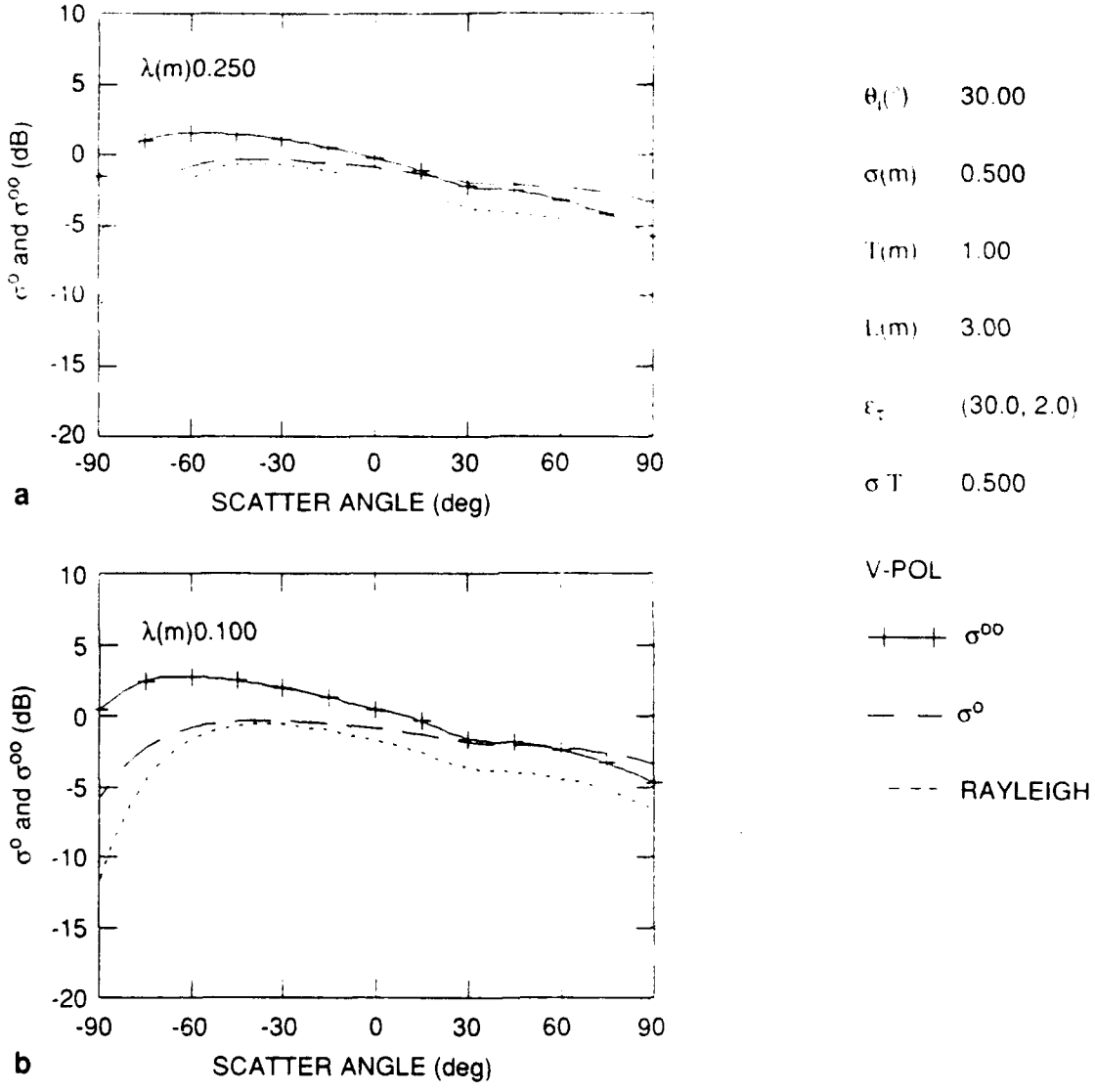

Figure 18. Mean and Variance of Scattered Power for:
a. $\theta_i = 30°$, $\lambda = 0.25$ m, $\sigma = 0.5$, $L = 3T$, $\varepsilon = 30 + j2$
b. $\theta_i = 30°$, $\lambda = 0.1$ m, $\sigma = 0.5$, $L = 3T$, $\varepsilon = 30 + j2$

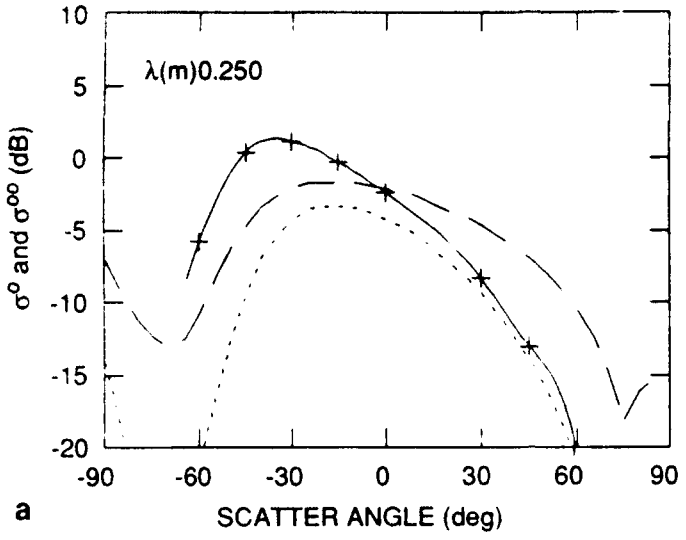

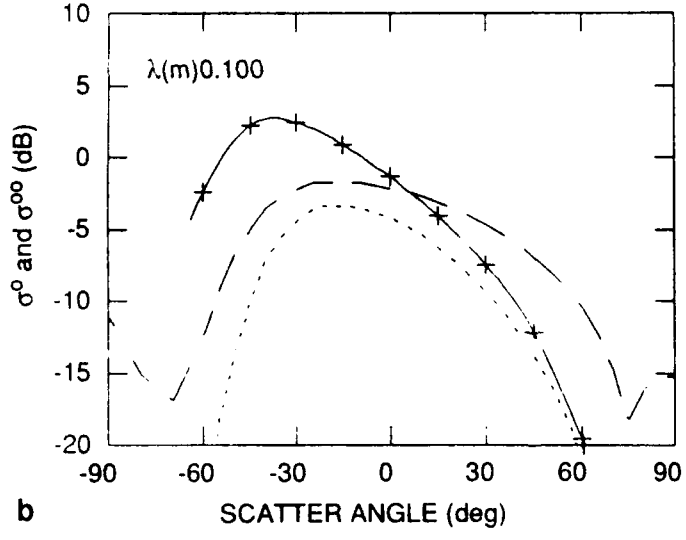

θ_i(°) 75.00

σ(m) 0.500

T(m) 1.00

L(m) 3.00

ε_r (30.0, 2.0)

σ/T 0.500

V-POL

σ°°

σ°

RAYLEIGH

Figure 19. Mean and Variance of Scattered Power for:
a. $\theta_i = 75°$, $\lambda = 0.25$ m, $\sigma = 0.5$, $L = 3T$, $\varepsilon = 30 + j2$
b. $\theta_i = 75°$, $\lambda = 0.1$ m, $\sigma = 0.5$, $L = 3T$, $\varepsilon = 30 + j2$

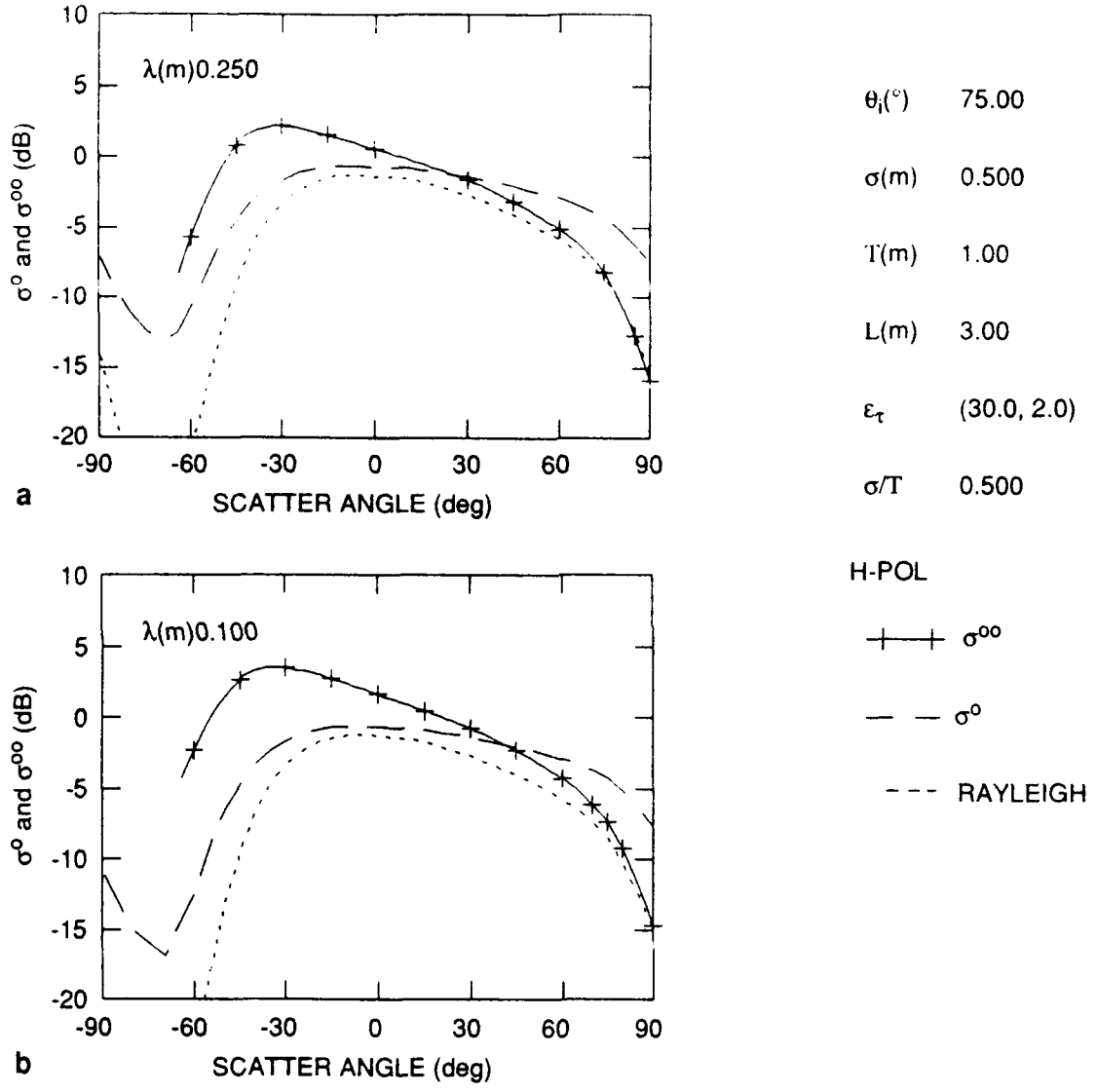

Figure 20. Mean and Variance of Scattered Power for H-pol for:
a. $\theta_i = 75°$, $\lambda = 0.25$ m, $\sigma = 0.5$, $L = 3T$, $\varepsilon = 30 + j2$
b. $\theta_i = 75°$, $\lambda = 0.1$ m, $\sigma = 0.5$, $L = 3T$, $\varepsilon = 30 + j2$

Figures 21 and 22 are plots of the normalized variance as a function of rms surface heights. These values are calculated by dividing the standard deviation by the mean value. Because the Rayleigh variance is defined as $\sigma^{oo} = (\sigma^o)^2$, a value of one means the variance is equal to the Rayleigh variance, while a value greater than one means the variance is larger than the Rayleigh value. These plots show that as θ_s approaches the backscatter region the variance is larger for the smoother surface. This is because the smoother surface will have so few facets with slopes large enough to cause backscatter that the small number of facets becomes the dominating factor in determining the scattering distribution for this region. In comparing Figures 21 and 22 it can also be seen that the variance is larger for $\theta_i = 75^o$. This would be expected because the slopes required to cause backscatter would have to be even steeper for this case. In the near specular and forward scatter regions, the scattering from the smoother surface is closer to Rayleigh than the rough surface scattering because there are many more facets oriented favorably to cause scattering in these regions.

Table 3 compares the calculated mean in the backscatter direction with measured values given by Ulaby[7] and Long.[2] The measured backscatter from soil given by Ulaby is compared to the calculated value for a dielectric constant of $\varepsilon_r = 30 + j2$. The measured backscatter from Arizona desert given by Long is compared to the backscatter calculated with $\varepsilon_r = 2 + j1.6$. Seawater measurements from Long are compared with calculations for $\varepsilon_r = 80 + j9$.

For the higher sea state calculation, corresponding to 16-ft waves, the shadowing function was included. For pure backscatter, $\theta_i = \theta_s$, the shadowing function is given as:[8]

$$S = (1 + C_2)^{-1}$$

where

$$C_2 = \left(\frac{4\sigma}{\pi T^2}\right)^{1/2} (\tan\theta_s) \exp\left(\frac{-T^2 \cot^2\theta_s}{4\sigma^2}\right) - \operatorname{erfc}\left(\frac{T \cot\theta_s}{2\sigma}\right). \tag{10}$$

For the parameters used in this calculation, one obtains S = 0.928. This means that even for high sea states at a 70° incident angle, shadowing is not a significant factor.

[7] Ulaby, F.T., Dobson, M.C. (1989) *Radar Scattering Statistics for Terrain*, Artech House, Dedham, Massachusetts.

[8] Sancer, M.I. (1969) Shadow Corrected Electromagnetic Scattering From a Randomly Rough Surface, *IEEE Trans. Antennas Propagat.*, **AP-17**:577-585.

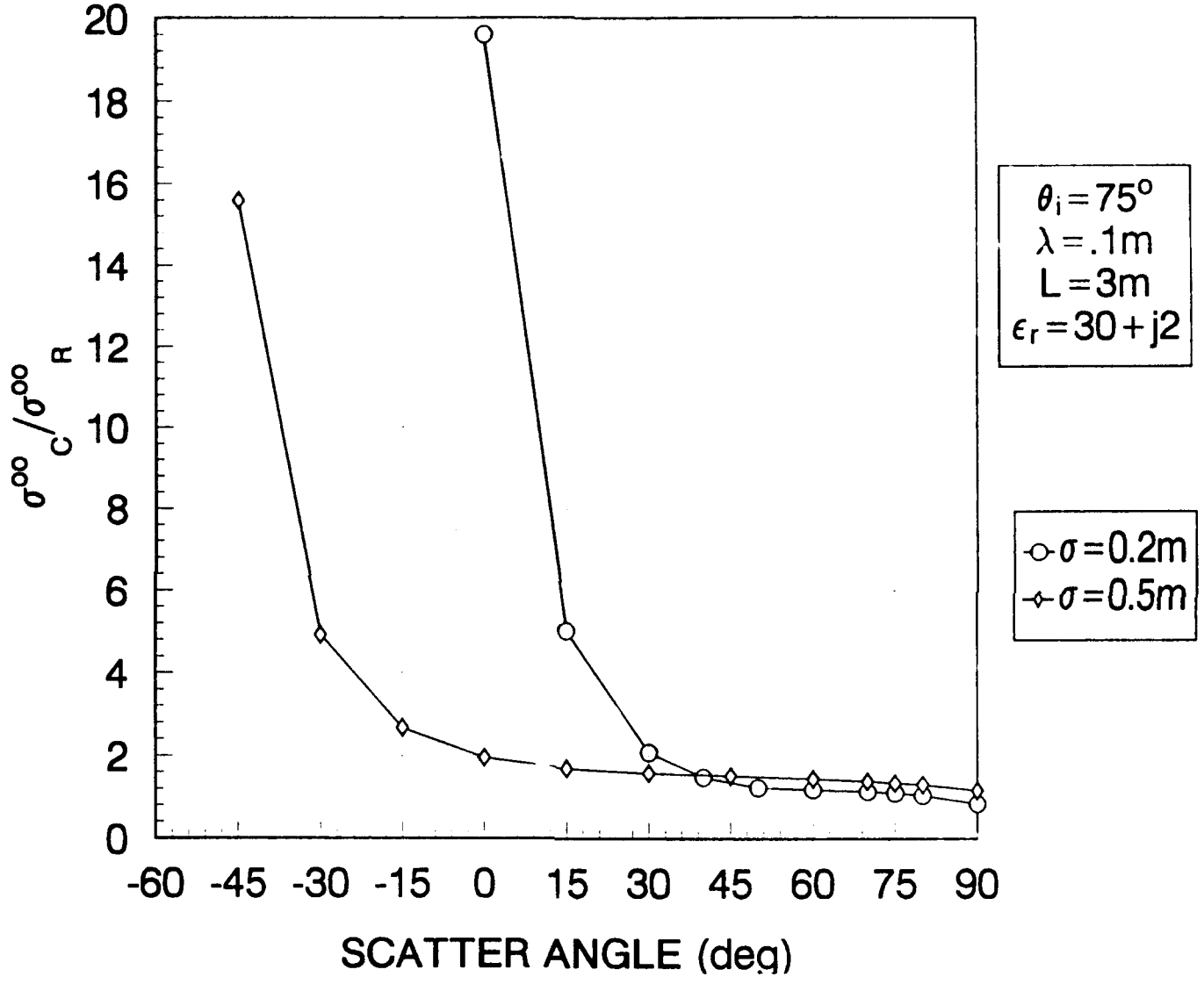

Figure 21. Comparison of Normalized Variance for Different Surface Roughness for $\theta_i = 75°$, $\lambda = 0.1$ m, $L = 3T$, $\varepsilon = 30 + j2$

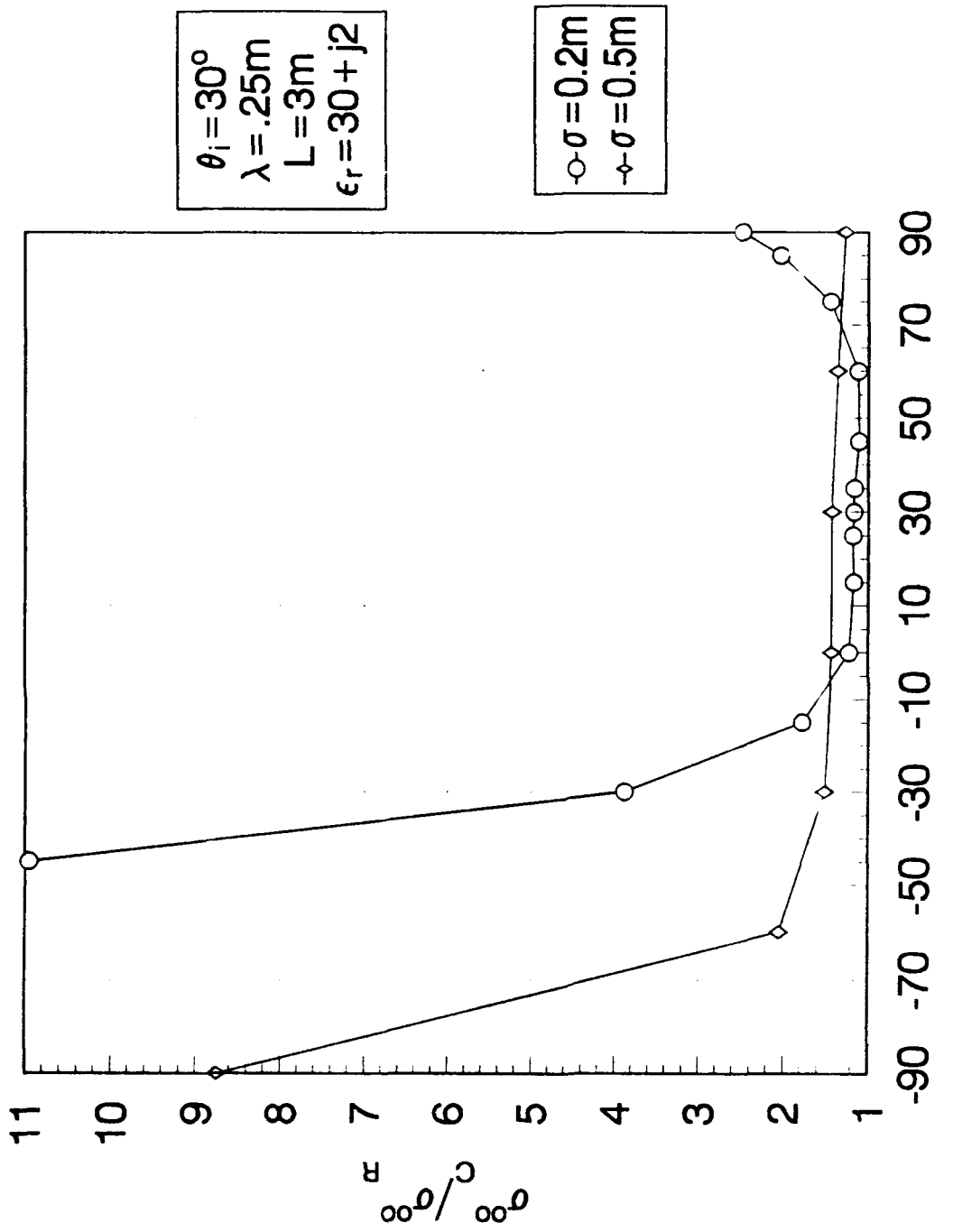

Figure 22. Comparison of Normalized Variance for Different Surface Roughness for $\theta_i = 30°$, $\lambda = 0.25$ m, $L = 3\Gamma$, $\varepsilon = 30 + j2$

Table 3. Comparison of Measured σ^o With Calculated σ^o.

ϵ_r	$\theta_{inc.}$	σ (m)	T (m)	L (m)	σ^o_{vv} calc.	σ^o_{vv} meas.
30 + j2	30°	.1	1	3	-15.96 dB	-13.9 dB
2 + j1.6	30°	.1	1	3	-23.61 dB	-25.75 dB
80 + j9	30°	.61	6	12	-19.94 dB	-20.0 dB
80 + j9	70°	1.225	6	18	-21.82 dB	-31.0 dB

For the given terrain surfaces, as well as the lower sea state, the agreement between calculations and measurements is extremely good. The calculation for the higher sea state, however, does not agree with the measured value, but this is not unexpected. High sea states do not have a Gaussian height distribution or a Gaussian correlation function, so the model used in this study cannot accurately describe scattering from very rough seas.

4. ARBITRARY LINEAR POLARIZATION

When the incident field is linearly polarized at some arbitrary angle, ψ, from the horizontal, the calculation of the reflection coefficient becomes somewhat more complicated. The incident linearly polarized wave can be separated into a horizontally polarized component and a vertically polarized component. The horizontal and vertical reflection coefficients and the magnitude of the overall reflection coefficient, $|R_{AL}|$ can then be calculated.

$$|R_{AL}| = \sqrt{\left(R_H R_H^*\right)\cos^2\psi + \left(R_v R_v^*\right)\sin^2\psi}\,. \tag{11}$$

The scattered field will no longer be linearly polarized but will have some ellipticity due to the unequal phase change of the horizontal and vertical components. The polarization of the scattered field can be found by examining the complex polarization factor, p, defined as:

$$p = \frac{E_v}{E_H} = \left|\frac{E_v}{E_H}\right| \cos\phi + j\left|\frac{E_v}{E_H}\right| \sin\phi \tag{12}$$

where: ϕ · phase difference between vertical and horizontal components of the scattered field

$$\text{Re (p)} = \left|\frac{E_v}{E_H}\right| \cos \phi$$

$$\text{Im (p)} = \left|\frac{E_v}{E_H}\right| \sin \phi.$$

The magnitude and phase of the components of the scattered field are determined directly from R_v and R_H. Table 4 shows the real and imaginary components of p for $\theta_i = 30°$, $\lambda = 0.1$ m, $\sigma = 0.2$ m, L = 3T, $\psi = 60°$, and $\varepsilon_r = 30 + j2$. The very small magnitude of Im (p) shows that the polarization of the scattered field is very close to linear. Case 2 is for $\varepsilon_r = 2 - j1.6$ with $\psi = 50°$. The scattered field in this case is slightly more elliptical due to the higher relative magnitude of the dielectric loss factor, ε'', but it is still highly linearly polarized. These two cases represent the highest degree of ellipticity for the values of p that were examined.

Table 4. Complex Polarization Factor

θ_s	Case 1		Case 2	
	Re (p)	Im (p)	Re (p)	Im (p)
-45	-1.7212	-0.0003	-1.1678	-0.0084
-30	-1.7321	0	-1.1918	0
-15	-1.7212	-0.0003	-1.1678	-0.0084
0	-1.6888	-0.0015	-1.0970	-0.0326
10	-1.6550	-0.0026	-1.0255	-0.0564
20	-1.6116	-0.0039	-0.9360	-0.0849
30	-1.5582	-0.0054	-0.8304	-0.1168
40	-1.6116	-0.0039	-0.9360	-0.0849
50	-1.6550	-0.0026	-1.0255	-0.0564
60	-1.6888	-0.0015	-1.0970	-0.0326
75	-1.7212	-0.0003	-1.1678	-0.0084
90	-1.7321	0	-1.1918	0

Im (p) = 0	Linear polarization	$p = \infty$	Vertical polarization
Im (p) > 0	Right elliptical polarization	p = 1	Right circular polarization
Im (p) < 0	Left elliptical polarization	p = -1	Left circular polarization
p = 0	Horizontal polarization		

Case 1: $\theta_i = 30°$, $\lambda = 0.1$ m, $\sigma = 0.2$ m, L = 3T, $\psi = 60°$, $\varepsilon_r = 30 + j2$
Case 2: $\theta_i = 30°$, $\lambda = 0.1$ m, $\sigma = 0.2$ m, L = 3T, $\psi = 50°$, $\varepsilon_r = 2 + j1.6$

Figures 23 through 25 show the mean and variance of the scattered power as the tilt angle ψ of the linear polarization increases. While the mean does decrease as the polarization goes from horizontal, $\psi = 0°$, through several values of ψ and finally to vertical polarization, $\psi = 90°$, the tilt angle of the polarization does not affect the Rayleighness of the statistics.

5. CONCLUSIONS

The main objective of this study was to determine whether cell size has any effect on the mean normalized cross section and variance of the scattered power from a rough surface. Several other variables were also studied including wavelength, dielectric constant, angle of incidence, surface roughness, and polarization.

Throughout the figures shown, several general trends can be seen. It is quite clear that the cell size does affect the scattering statistics. For the largest cell size, L = 12T, the calculated value of σ^{oo} is almost an exact match to the Rayleigh value of σ^{oo} over the entire range of scattering angles. As the size of the cell decreases, the variance of the scattered power becomes larger than the Rayleigh variance, especially in the backscatter region, due to fewer facets scattering in this direction. This means that the problem of non-Rayleigh scattering for finite clutter cells is a more significant problem for monostatic radar systems than for large angle bistatic radars.

The wavelength also affects the statistics of the scattered power for a surface containing many scatterers. As the wavelength increases, the Rayleigh parameter, Σ, decreases and the surface becomes less rough, so that the scattering is closer to Rayleigh.

Other parameters such as dielectric constant and tilt angle of the incident polarization affect the mean value of the scattered field, but do not affect the Rayleighness of the scattered field.

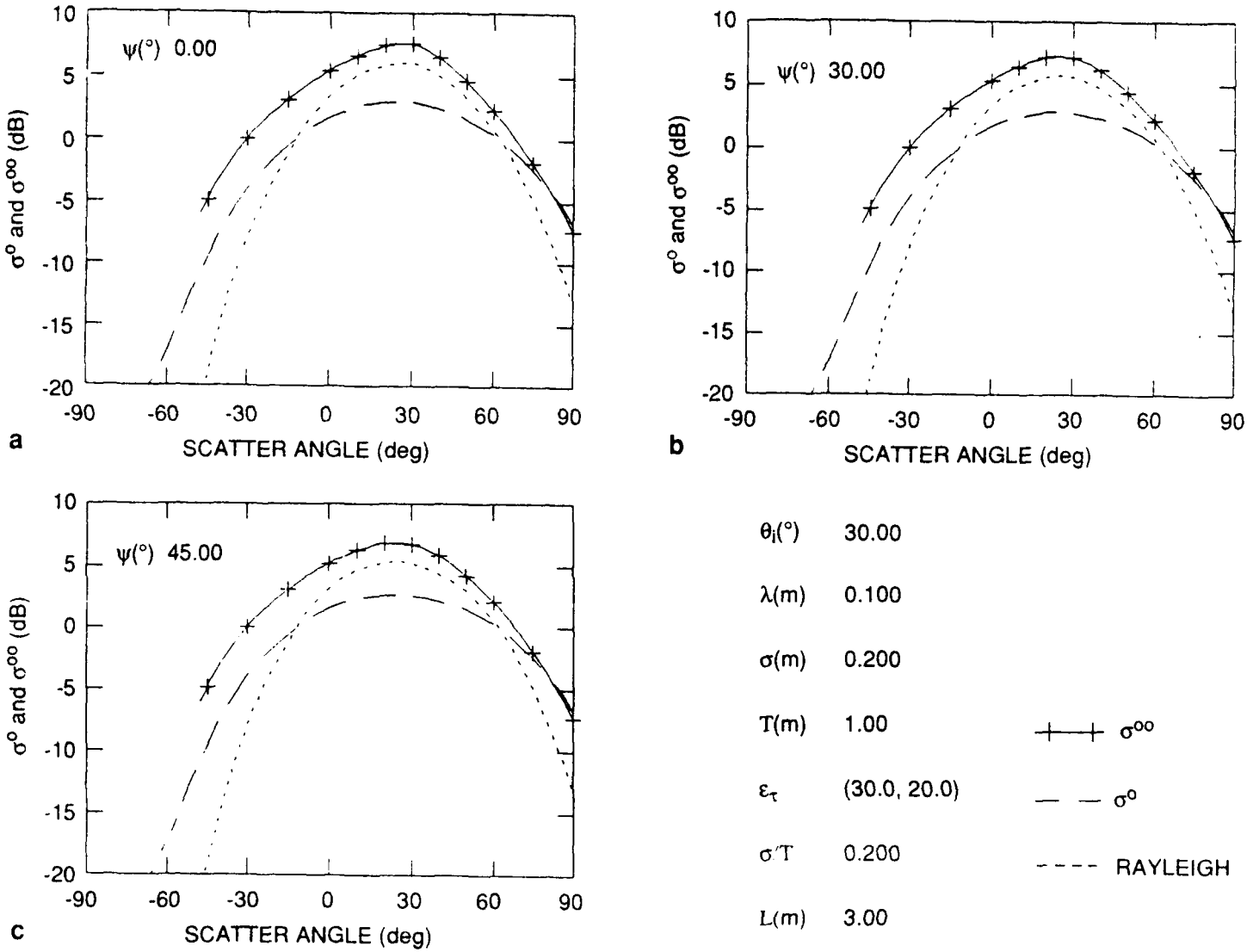

Figure 23. Mean and Variance of Scattered Power for:
a. $\theta_i = 30^o$, $\lambda = 0.1$ m, $\sigma = 0.2$, $L = 3T$, $\varepsilon = 30 + j2$, $\psi = 0^o$
b. $\theta_i = 30^o$, $\lambda = 0.1$ m, $\sigma = 0.2$, $L = 3T$, $\varepsilon = 30 + j2$, $\psi = 30^o$
c. $\theta_i = 30^o$, $\lambda = 0.1$ m, $\sigma = 0.2$, $L = 3T$, $\varepsilon = 30 + j2$, $\psi = 45^o$

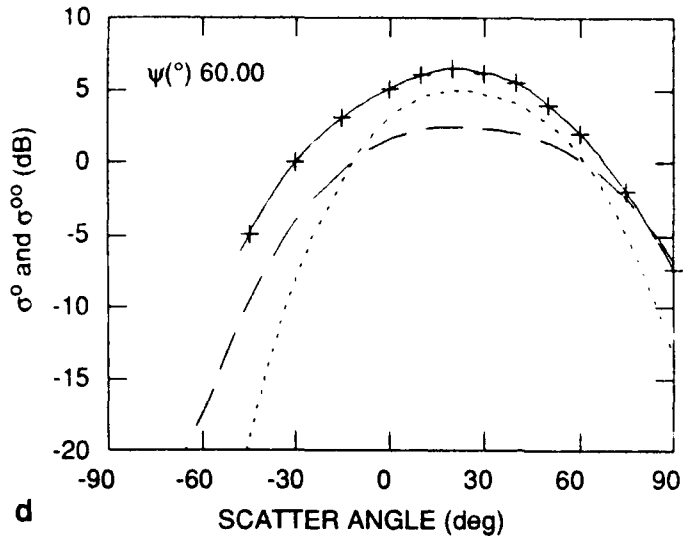

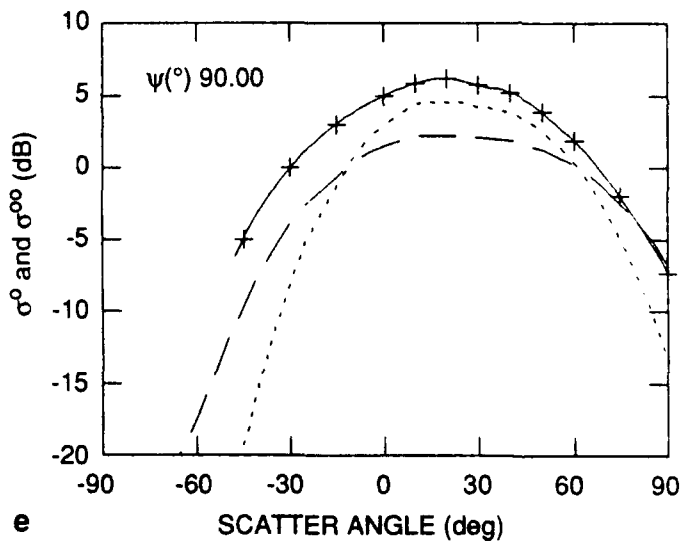

θ_i(°) 30.00

λ(m) 0.100

σ(m) 0.200

Γ(m) 1.00

ε_τ (30.0, 2.0)

σ/T 0.200

L(m) 3.00

σ°°

σ°

RAYLEIGH

Figure 23. Mean and Variance of Scattered Power for:
d. $\theta_i = 30°$, $\lambda = 0.1$ m, $\sigma = 0.2$, $L = 3T$, $\varepsilon = 30 + j2$, $\psi = 60°$
e. $\theta_i = 30°$, $\lambda = 0.1$ m, $\sigma = 0.2$, $L = 3T$, $\varepsilon = 30 + j2$, $\psi = 90°$

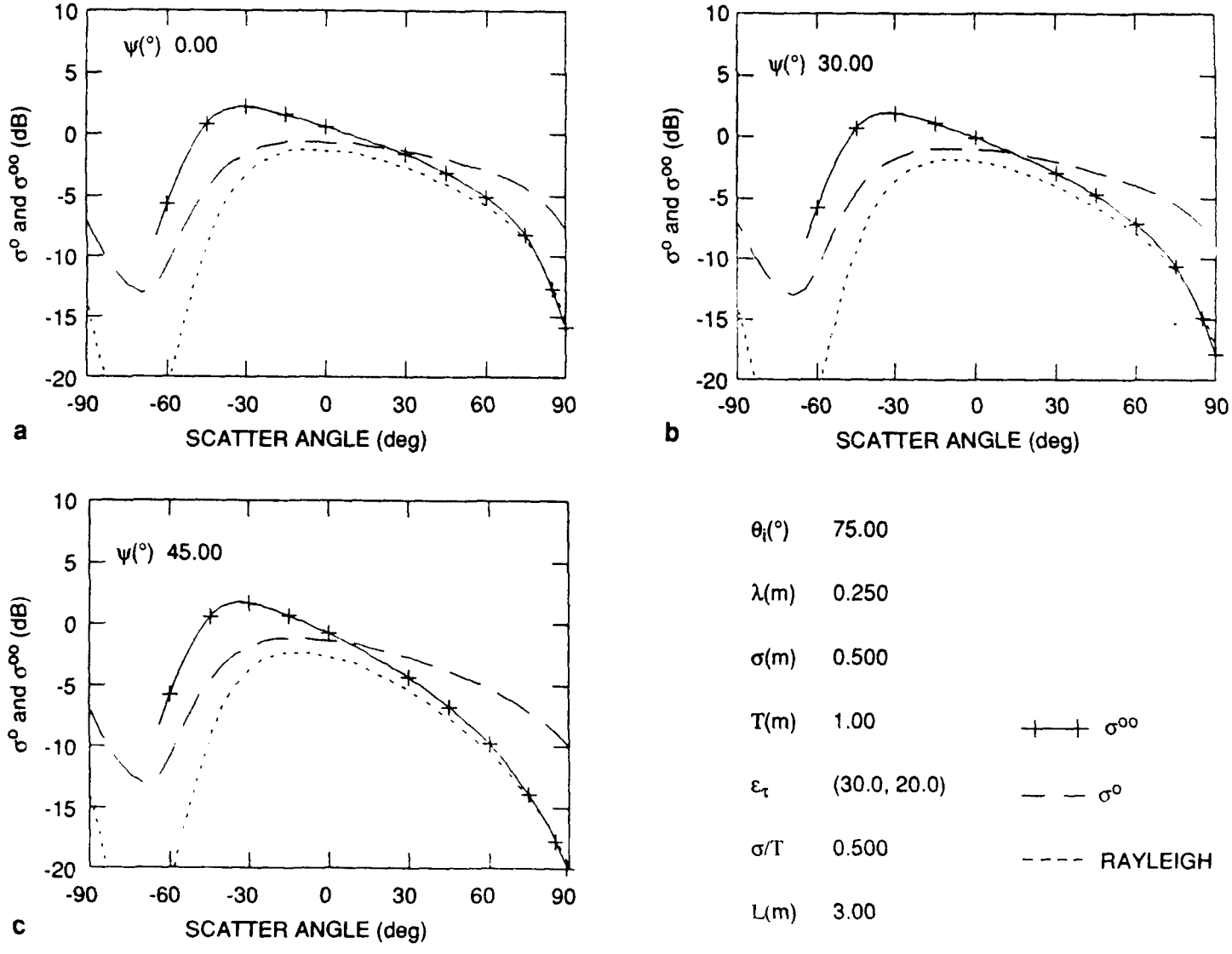

Figure 24. Mean and Variance of Scattered Power for:
a. $\theta_i = 75^o$, $\lambda = 0.25$ m, $\sigma = 0.5$, $L = 3T$, $\varepsilon = 30 + j2$, $\psi = 0^o$
b. $\theta_i = 75^o$, $\lambda = 0.25$ m, $\sigma = 0.5$, $L = 3T$, $\varepsilon = 30 + j2$, $\psi = 30^o$
c. $\theta_i = 75^o$, $\lambda = 0.25$ m, $\sigma = 0.5$, $L = 3T$, $\varepsilon = 30 + j2$, $\psi = 45^o$

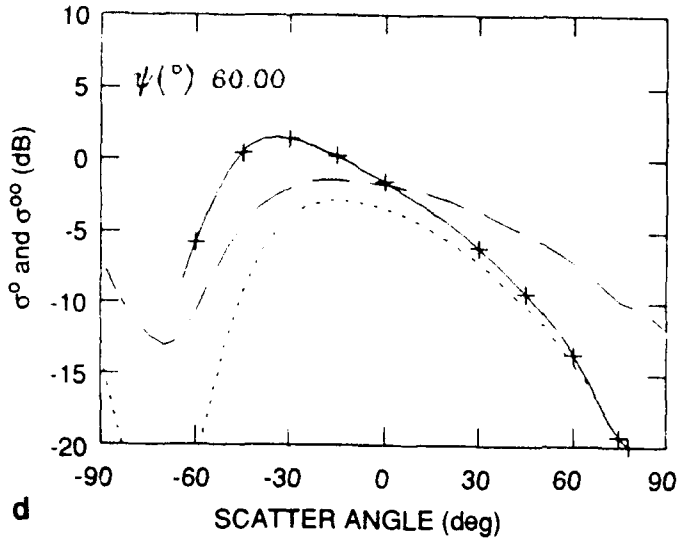

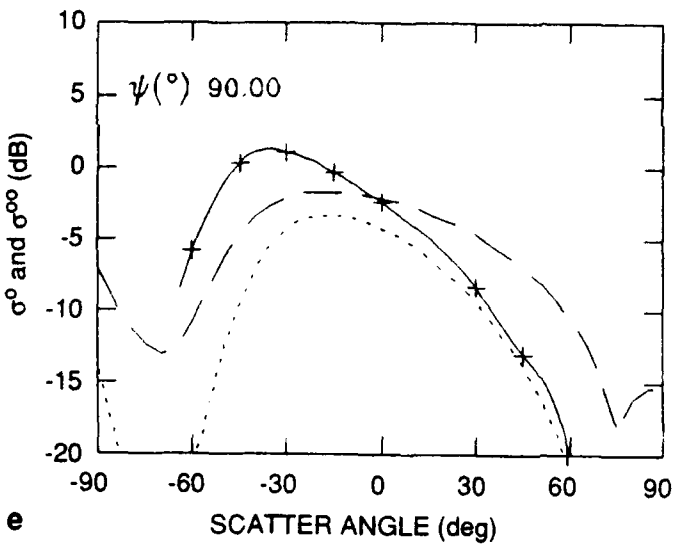

θ_i(°)	75.00
λ(m)	0.250
σ(m)	0.500
T(m)	1.00
ε_r	(30.0, 2.0)
σ/T	0.500
L(m)	3.00

+—+ σ^{oo}

— — σ^{o}

- - - RAYLEIGH

Figure 24. Mean and Variance of Scattered Power for:
d. $\theta_i = 75°$, $\lambda = 0.25$ m, $\sigma = 0.5$, $L = 3T$, $\varepsilon = 30 + j2$, $\psi = 60°$
e. $\theta_i = 75°$, $\lambda = 0.25$ m, $\sigma = 0.5$, $L = 3T$, $\varepsilon = 30 + j2$, $\psi = 90°$

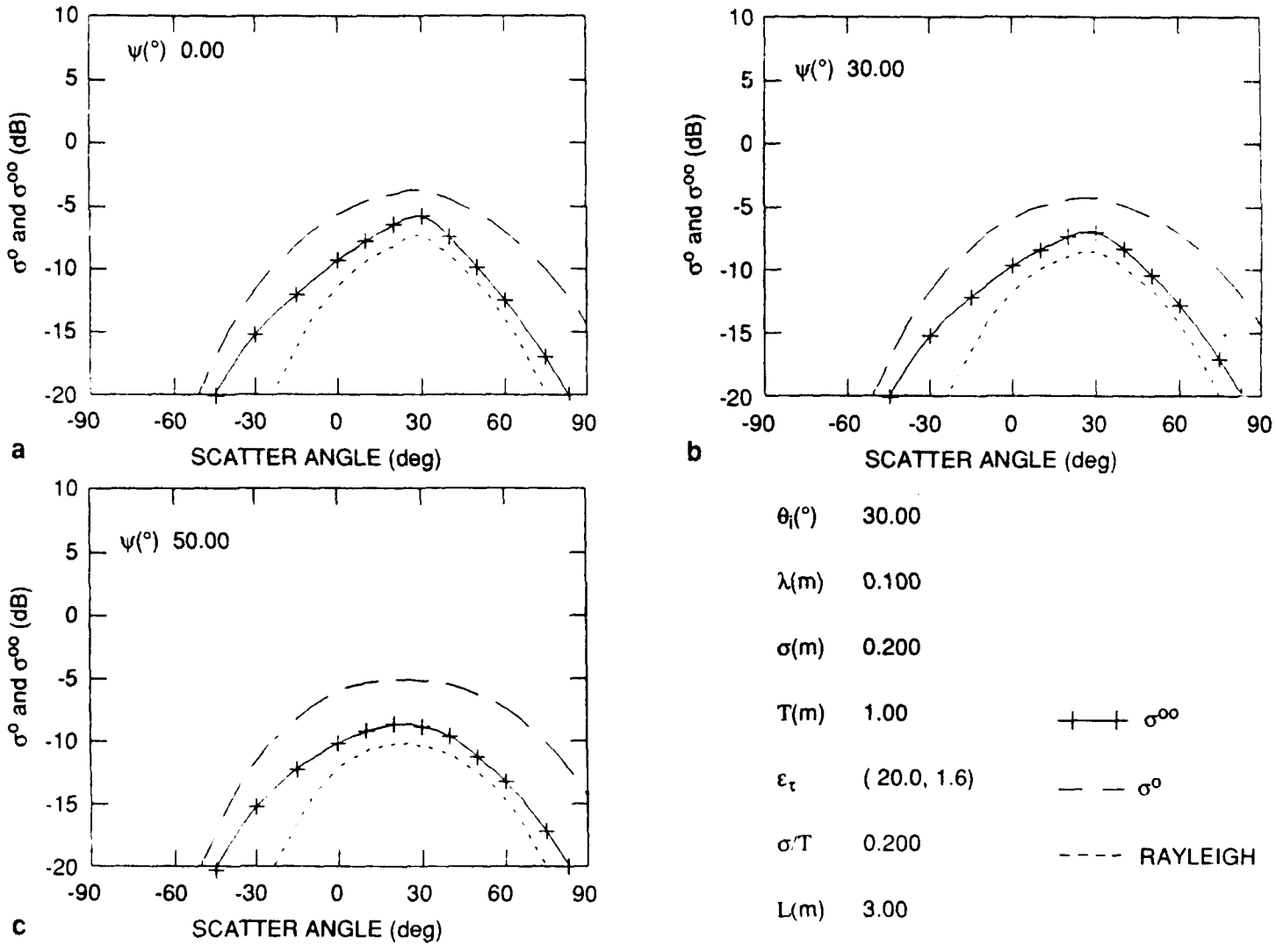

Figure 25. Mean and Variance of Scattered Power for:
a. $\theta_i = 30^o$, $\lambda = 0.1$ m, $\sigma = 0.2$, $L = 3T$, $\varepsilon = 2 + j1.6$, $\psi = 0^o$
b. $\theta_i = 30^o$, $\lambda = 0.1$ m, $\sigma = 0.2$, $L = 3T$, $\varepsilon = 2 + j1.6$, $\psi = 30^o$
c. $\theta_i = 30^o$, $\lambda = 0.1$ m, $\sigma = 0.2$, $L = 3T$, $\varepsilon = 2 + j1.6$, $\psi = 50^o$

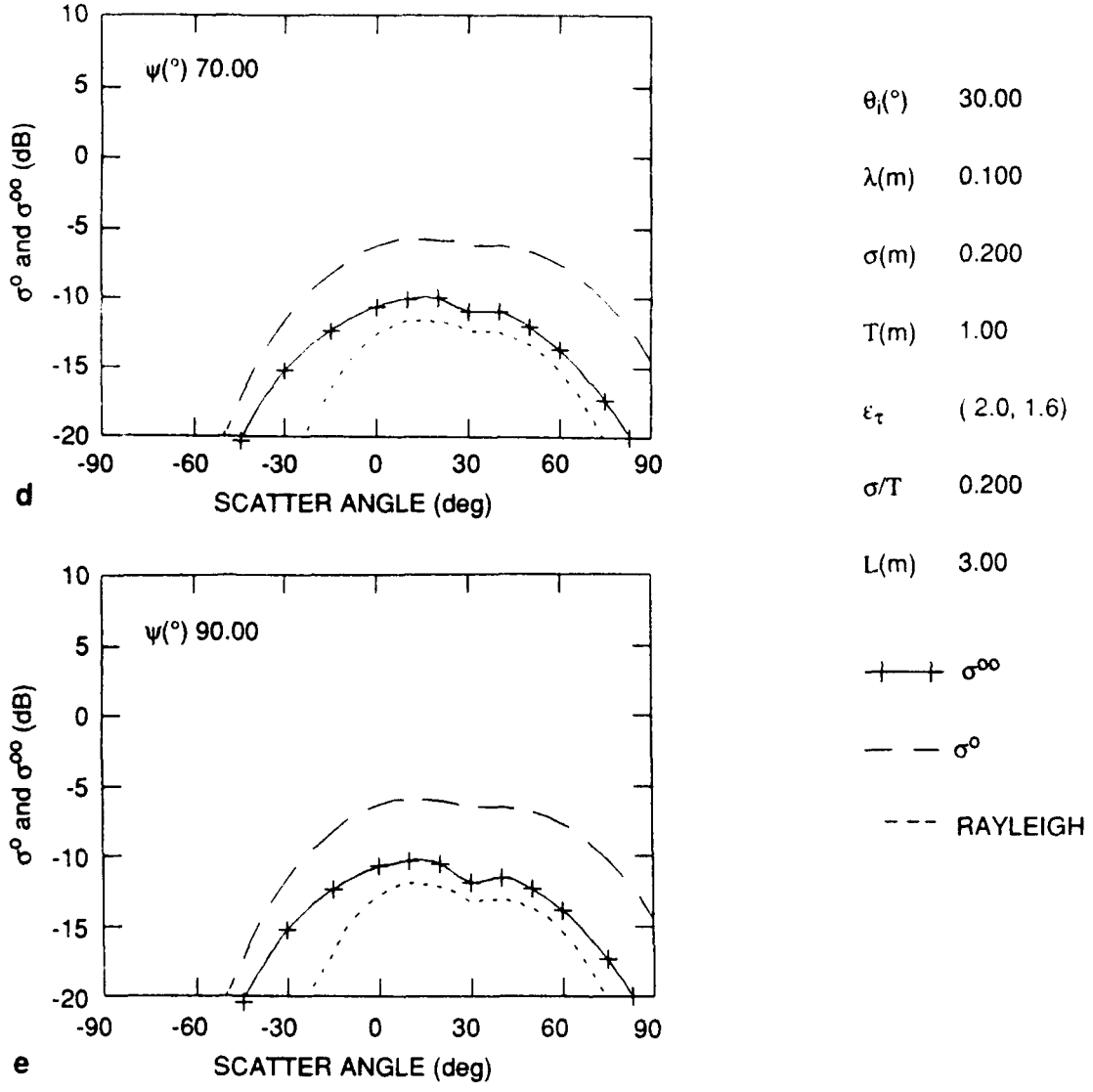

Figure 25. Mean and Variance of Scattered Power for:
d. $\theta_i = 30°$, $\lambda = 0.1$ m, $\sigma = 0.2$, $L = 3T$, $\varepsilon = 2 + j1.6$, $\psi = 70°$
e. $\theta_i = 30°$, $\lambda = 0.1$ m, $\sigma = 0.2$, $L = 3T$, $\varepsilon = 2 + j1.6$, $\psi = 90°$

References

1. Skolnik, M.I. (1980) *Introduction to Radar Systems*, McGraw-Hill Book Company, New York.

2. Long, M.W. (1975) *Radar Reflectivity of Land and Sea*, D.C. Heath and Company, Lexington, MA.

3. Papa, R.J., and Woodworth, M.B. (1991) *The Mean and Variance of Diffuse Scattered Power as a Function of Clutter Resolution Cell Size*, RADC-TR-91-09.

4. Beckmann, P., and Spizzichino, A. (1963) *The Scattering of Electromagnetic Waves from Rough Surfaces*, The MacMillan Co., New York.

5. Ruck, G.T., Barrick, D.E., Stuart, W.D., and Krichbaum, C.K. (1970) *Radar Cross Section Handbook*, Vol. 2, Plenum Press, New York.

6. Papoulis, A. (1965) *Probability, Random Variables, and Stochastic Processes*, McGraw-Hill Book Company, New York.

7. Ulaby, F.T., Dobson, M.C. (1989) *Radar Scattering Statistics for Terrain*, Artech House, Dedham, Massachusetts.

8. Sancer, M.I. (1969) Shadow Corrected Electromagnetic Scattering From a Randomly Rough Surface, *IEEE Trans. Antennas Propagat.*, **AP-17**:577-585.